Title	Studies on responses induced by phospholipid nanoparticles in mammalian cells
Author(s)	藤田, 和代
Citation	大阪大学, 2020, 博士論文
Version Type	VoR
URL	https://doi.org/10.18910/76394
rights	
Note	

Studies on responses induced by phospholipid nanoparticles in mammalian cells

Doctoral thesis

Kazuyo Fujita

Department of biological science

Graduate school of science

Osaka University

要旨

　リン脂質は水溶液中で脂質二重膜構造を持つ小粒子を形成する性質を持っているので、これを利用して人工的に調製したリン脂質ナノ粒子（phospholipid nanoparticles：PNPs）がリポソームである。リポソームは内部や膜に薬剤などの物質を保持できることから、drug delivery system （DDS）の搬送体の一つとして広く利用されている。また、生体内で細胞から放出される細胞外小胞の一種であるエクソソームも PNPs の一種であるが、脂質、核酸、タンパク質などの生理活性物質を運搬することにより細胞間の情報伝達に関与していることが近年明らかにされている。しかし、これら PNPs 自体が細胞に取り込まれた場合、細胞にどのような影響を及ぼすのかについては未だに不明な点が多い。そのため PNPs が細胞に及ぼす影響について、その作用機序も含めて明らかにすることを目的として本研究を開始した。

　これまでに PNPs がマクロファージに取り込まれると脂肪滴（lipid droplets：LDs）の形成が誘導されることが報告されている。LDs はトリアシルグリセロール等を含有することからエネルギー貯蔵の小器官と考えられてきたが、他にも多様な機能を有していることが明らかになっている。しかし、マクロファージ以外の哺乳動物細胞で PNPs により LDs が誘導されるのかどうかについてはわかっていなかった。そこで本研究では先ず PNPs による非マクロファージ系細胞でマクロファージと同様に LDs が誘導できるかどうかについて検討した。LDs はナイルレッド染色した後、flow cytometer により定量解析した。ヒト胎児腎細胞由来の HEK293T 細胞株や様々な哺乳動物由来細胞株に PNPs を加えて培養を行ったところ、マクロファージと同様に細胞内に LDs が誘導された。LDs の誘導活性はリポソームの脂質の組成によって異なっており、dioleoyl-phosphatidylcholine（DOPC）のみで作成したリポソームや DOPC と dioleoyl-phosphatidylethanolamine（DOPE）を混合して作製した DOPC/DOPE リポソームよりも DOPC と dioleoyl-phosphatidylserine（DOPS）を混合して作製した DOPC/DOPS リポソームを用いた方が強い LD 誘導活性がみられたことから、リン脂質の中でも PS に強い LD 誘導活性があることがわかった。さらにウシミルクから精製したエクソソームでも同様に LDs の誘導作用が認められたが、ポリスチレンビーズでは LDs 誘導活性がみられなかった。これらの結果から、LDs の誘導は PNPs の特性の一つであることが示唆された。透過型電子顕微鏡を用いて LDs の観察をおこなったところ、リポソームによって誘導された LDs は比較的低電子密度の均一構造を持つ粒子として細胞質内に分布していることがわかった。これまではマクロファージでのみ報告されていた PNPs による LDs の誘

1

導現象は、幅広い哺乳動物細胞に共通して見られる PNPs に対する細胞の応答現象であることを初めて明らかにすることができた。

　また、HEK293T 細胞へのリポソームの取り込み量について調べたところ、DOPC/DOPE リポソームの取り込み（endocytosis）が非常に高いことがわかった。しかし、DOPC のみのリポソームや DOPC/DOPS リポソームの取り込みは低かった。これらの結果から HEK293T 細胞には DOPC/DOPE リポソームの取り込みを促進する PE 受容体が高発現していることが推定された。そこで PE 受容体を特定するため、HEK293T 細胞の網羅的遺伝子発現解析をおこない、高発現している 4 種類の受容体候補遺伝子を得た。HEK293T 細胞をこれらの候補遺伝子に対する siRNA で処理し、リポソームの取り込みを調べたところ、high density lipoprotein（HDL）の受容体として知られている scavenger receptor class B type 1（SR-B1）に対する siRNA で最も強く取り込みが抑制された。また、SR-B1 発現プラスミドを導入して SR-B1 を過剰発現させた HEK293T 細胞では、PE 含有リポソームの取り込みが顕著に増加した。さらに抗 SR-B1 抗体は HEK293T 細胞での PE 含有リポソームの取り込みを阻害した。細胞内に取り込まれた PE 含有リポソームは、endosomes/lysosomes および SR-B1 と共局在していることが共焦点レーザー顕微鏡での観察によって確認できた。これらの結果から、SR-B1 は PE 受容体として PE 含有リポソームの endocytosis を誘導し、リポソームは SR-B1 と共に endosomes/lysosomes に取り込まれることを初めて明らかにすることができた。

　PNPs による LDs の誘導実験を行う過程で、細胞に PE 含有リポソーム等を作用させると LDs が誘導されるだけでなく、グルコース欠乏条件で培養したマウス繊維芽細胞由来 L929 細胞株に対して生存延長作用を有することがわかった。PNPs による LDs の誘導は栄養欠乏状態での細胞の生存に影響を与えることが示唆された。

　以上の研究により、哺乳動物細胞では PNPs に対する共通の応答として LDs 形成が誘導されることを明らかにした。PNPs の中で PE 含有リポソームの Endocytosis の機構を詳細に調べた結果、SR-B1 を介して受容体依存的に取り込まれて LDs を誘導することが分かった。本研究により、哺乳動物細胞にはこのような PNPs に対する一連の応答機構が存在することを初めて明らかにすることができた。

Chapter I
General Introduction

Chapter II
Induction of lipid droplets in non-macrophage cells as well as macrophages by liposomes and exosomes

Chapter III
SR-B1 acts as a receptor for the endocytosis of phosphatidylethanolamine-containing liposomes

Chapter IV

Effect of liposomes on cell survival under glucose-deficient conditions

Chapter V

Chapter I
General Introduction

1.1. Phospholipid nanoparticles

As phospholipids are amphiphilic molecules possessing hydrophilic headgroups attached to nonpolar long hydrocarbon chains, they form a lipid bilayer in an aqueous solution through self-assembly. In 1964, English hematologist Alec Bangham demonstrated for the first time that small artificial particles could be produced using phospholipids [1], and these phospholipid nanoparticles (PNPs) have lately been referred to as liposomes [2]. Liposomes are therefore artificial PNPs and they have been considered simple models mimicking cell membranes. they were initially used to analyze biological and molecular properties of cell membranes.

A variety of phospholipids and their derivatives are used to prepare liposomes. Major phospholipids of mammalian cell membranes are frequently used as constituents of liposomes, e.g., phosphatidylcholine (PC), phosphatidylethanolamine (PE), phosphatidylserine (PS), phosphatidic acid (PA), and phosphatidylinositol (PI). In an aqueous solution at pH 7, PC and PE are almost neutral whereas PS, PA, and PI are negatively charged. In addition, the molecular shape of these phospholipids in water is not identical: PC and PE show cylinder and cone shapes, respectively. Therefore, the combination of phospholipids and their derivatives generates divergently different properties of liposomes. Cholesterol, a major lipid as well as phospholipids in cell membranes, is also used together with phospholipids to prepare liposomes. Addition of cholesterol influences liposomal stability by its rigidizing effect on the phospholipid bilayer [3, 4].

Recently, liposomes have attracted attention as carriers in drug delivery system (DDS) because they can contain targeted substances (e.g., small molecular drugs, proteins, siRNAs, and DNAs) in their aqueous cores or membranes. Although liposomes have primarily excellent properties as carriers of various substances with respect to biocompatibility and capability of loading or releasing various substances, the recent development of various liposomal technologies has enabled the clinical application of

liposomes. Technological breakthroughs including the following points have drastically improved the usefulness of liposomes as carriers [5, 6].

(1) Improvement of liposomal stability in circulation

When simple liposomes consisting of phospholipids are administered in vivo, they are unstable and immediately trapped in the reticular endothelial system. To avoid the rapid clearance of liposomes after administration in vivo, adequate liposomal compositions and sizes have been investigated, although longer-circulating liposomes are not always required in some cases. Smaller, uncharged liposomes are more stable than large, charged liposomes in systemic circulation. Furthermore, coating of liposomes by hydrophilic polymers such as polyethylene glycol (PEG) can prevent the rapid liposomal uptake by the reticular endothelial system. This type of liposomes is referred to as stealth liposomes. To deliver liposomes into solid tumors, longer-circulating liposomes are advantageous because these liposomes are expected to accumulate around solid tumors by the effect of enhanced permeation and retention (EPR) based on the vulnerability of tumor vasculature generated by angiogenesis [7].

(2) Active targeting

Surface modification of liposomes has been conducted to accumulate liposomes efficiently for target cells and tissues. To achieve active targeting, antibodies and ligands are conjugated to liposomes. Antibody-conjugated PEGylated liposomes have been developed for the use of cancer therapy. As transferrin receptors are abnormally expressed on various cancers, transferrin-conjugated liposomes have been examined for imaging and cancer therapy. In addition, some peptides including RDG have been employed as ligands to conjugate to liposomes. Side effects of anti-cancer drugs can be reduced by encapsulating the drugs in the liposomes [8].

(3) Other technologies

To achieve high loading efficacy of substances into liposomes, a remote-loading method has been invented. By this method, some drugs in the external phase of liposomes can be encapsulated very efficiently into liposomes through a pH gradient. Usually, liposomes are uptaken into mammalian cells by endocytosis and then these are delivered into the endosomes/lysosomes. In the endosomes/lysosomes, liposomes are degraded by various digestive enzymes including lipases, proteases, and nucleases. In the case of degradable payloads by these enzymes, such as nucleic acids and proteins, escape from

endosomes/lysosomes and rapid cytoplasmic delivery is critical for expressing their activities. Liposomes containing fusogenic lipids and pH-sensitive or cell-penetrating peptides, which can disrupt endosomes, have been explored for the efficient delivery of payload in the liposomes to the cytoplasm, although cytoplasmic delivery is still a crucial issue to be resolved [7, 8].

Natural PNPs exist in body fluid. Extracellular vesicles (EVs) are phospholipid particles released from cells. EVs exist in most body fluids including blood, saliva, urine, milk, amniotic fluid, and cerebrospinal fluid. Although EVs were once considered to be a type of cell debris, experimental artefacts, and waste, recent studies have revealed that these play crucial roles in intercellular communication by transferring bioactive substances such as nucleic acids, proteins, and lipids. Although there is no consensus on a clear definition for each type of EV at this moment, EVs have been classified into the following different sub-types based on their origins and sizes. (1) Exosomes are natural PNPs (40-100 nm) derived from endosomes released into the extracellular environment through the fusion of cell membranes and cytoplasmic multivesicular bodies encapsulating multiple endosomes. (2) Microvesicles (100-1000 nm) are produced by the budding of cell membranes. (3) Apoptotic bodies (>800 nm) are formed by vesicles bulging out from the cell membrane of a dying cell during the apoptotic process [13].

Although exosomes were originally discovered in animals [14], similar PNPs are also found in plants including fruits and vegetables [15]. Exosomes contain a variety of substances including lipids, proteins, carbohydrates, and nucleic acids[16]. As the component of the lipid bilayer, exosomes include cholesterol, sphingomyelin, PC, PS, and PE, which are typical lipid components of cell membranes, although the ratio of these components differs considerably between exosomes and parental cells. It is pointed out that the lipid composition of exosomes is similar to those of membrane raft and HIV particles with respect to enrichment of cholesterol and sphingomyelin [17]. Contents of exosomes vary depending on parental cell conditions in normal or disease state. Exosomes are therefore useful as diagnostic biomarkers [18].

Although carrier functions of PNPs appear to be a main subject of recent interest, the biological actions of PNPs themselves on mammalian cells might not have been studied thoroughly. I believe that the understanding of cellular responses to PNPs themselves and these mechanisms are very important in both aspects of basic and applied bioscience.

Therefore, in this thesis, I investigated a general cellular response to PNPs and found that lipid droplet (LD) formation is a response to PNPs found in a variety of mammalian cells, not only macrophages but also non-macrophage cells. I described the study on LD induction of cells by PNPs in Chapter II. Through the studies in this thesis, I found that PNPs consisting of various phospholipids would be incorporated into cells via different pathways, although some pathways might overlap. I succeeded in identifying a pathway in which phosphatidylethanolamine (PE)-containing liposomes are endocytosed into cells via a receptor. I described this study on identification of a liposomal receptor in Chapter III. In Chapter IV, I explained our findings that liposomal treatment promotes cell survival under glucose-deficient culture conditions (Fig. 1).

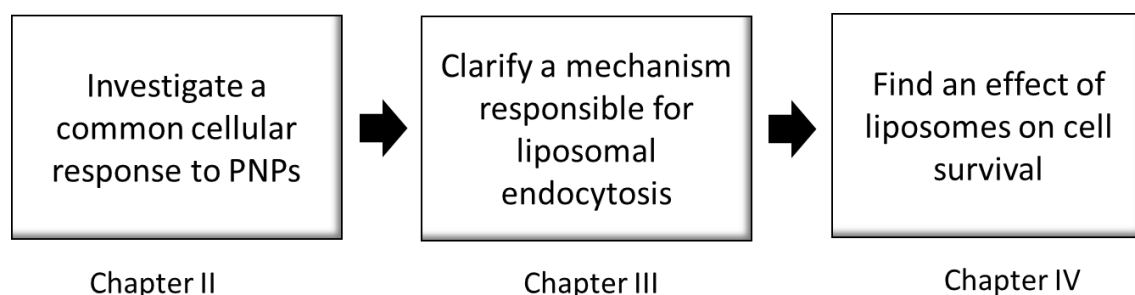| Investigate a common cellular response to PNPs	→	Clarify a mechanism responsible for liposomal endocytosis	→	Find an effect of liposomes on cell survival
Chapter II		Chapter III		Chapter IV

Fig. 1 flow of studies in this thesis

1.2. Lipid droplets

Lipid droplets (LDs) are ubiquitous intracellular organelles found not only in animals but also in plants, fungi, and bacteria [22]. Although LDs mainly contain triacylglycerol (TAG) and cholesteryl ester, more than 100 different molecular species of neutral lipids are detected in LDs. Some fat-soluble vitamins and their metabolites including vitamin E (tocopherol) and vitamin A (retinol) are also stored in LDs. In addition, the precursors of eicosanoids including prostaglandins, thromboxanes, and leukotrienes are detected in LDs. These facts indicate that LDs contribute to metabolic and signaling regulation in cells [23]. The core of LD is surrounded by a monolayer of phospholipids. The most abundant phospholipid is PC, followed by PE and PI. Specific proteins such as perilipins

1-5 are integrated into the phospholipid monolayer. Perilipins protect the degradation of LDs from lipase; however, depending on the circumstances, these molecules facilitate lipolysis of LDs by controlling the access of lipase and its co-factor [24]. As a model of LD formation, LDs are considered to generate from the endoplasmic reticulum (ER) membrane through a budding-like process [25]. Nowadays LDs are known to have multifunctions as summarized below.

(1) Energy storage

Initially, LDs had been considered to be simple fatty storage organelles. TAG in the core of LDs is utilized during the deficiency of nutrients or cell growth [26]. Lipolysis and lipophagy are two catabolic pathways of TAG in LDs. Fatty acids (FAs) are produced from catabolized TAG and these are the most efficient substrates for cells to generate energy through beta-oxidation. However, free FAs are toxic substances to cells, because they can act as detergents. Therefore, in contrast, it can be said that LDs have a function to prevent the lipotoxicity of free FAs by incorporating these toxic substances [23, 25].

(2) Response to stress

Various changes in LDs are found in some diseases including cancer, hepatic steatosis, and atherosclerosis. In addition, LDs increase in response to various stresses such as excess FAs, nutrient deficiency, and/or redox imbalance. Endoplasmic reticulum stress, which is caused by the imbalance of unfolded proteins and chaperones, also induces LDs through unfolded protein response (UPR)-dependent mechanisms. In addition, oxidative stress caused by hypoxia, oxidants, mitochondrial impairment, and ER stress induces the accumulation of LDs. Signaling pathways of oxidative and ER stress sometimes influence and connect each other. Although entire mechanisms are still under investigation, LDs can function to mitigate these stresses [23].

(3) Regulation of proteins

LDs play a regulatory role in the maturation and folding of some proteins. In the production of hepatitis C virus, LDs are related to maturation and the assembly of viral proteins. LDs are also associated to the maturation of other viruses (e.g., dengue virus, bovine viral diarrhea virus, and bunya virus). LDs can store nuclear proteins (histones) including H2A, H2Av, and H2B. These histones are retained in LDs by an anchor substance. LD histones take part in early development and innate immunity. In the turnover of various proteins, LDs act as a platform to proceed degradation. For example,

9

in degradation processes, apolipoprotein B (ApoB) or 3-hydroxy-3-methyl-glutaryl-coenzyme A (HMG-CoA) reductase is transferred to LDs. These proteins are ubiquitinated and then degraded by the proteasome system [23].

Regarding the relation of PNPs and LDs, endocytosis of PNPs has been reported to induce LDs in macrophages [26, 27]. However, it has not been clarified whether the formation of LDs is a common cellular response to liposomes in most mammalian cells involving not only macrophages but also other types of cells. During my previous study to examine the effects of liposomes on non-macrophage cells [28, 29], I noticed that treatment with liposomes could induce a morphological change in which granule-like structures appeared in the cytoplasm (Fig. 2). Later, these cytoplasmic granules were found to be LDs. These findings led to initiate the studies of this thesis.
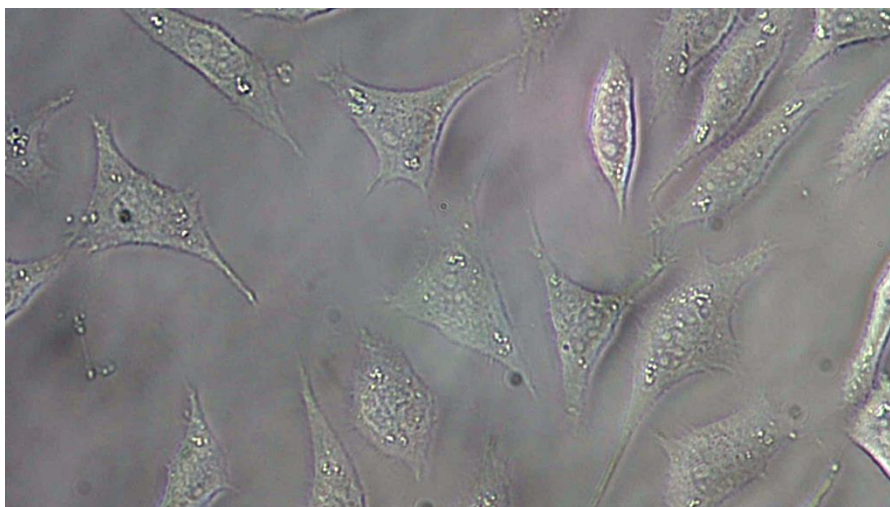

Fig. 2 Observation of glandular structures induced by liposomal treatment in a mouse fibroblastic cell line L929

1.3. Scavenger receptor class B type 1

Scavenger receptors were originally reported as receptors capable of recognizing modified low-density lipoproteins (LDL). Currently, scavenger receptors are defined as cell surface receptors, which are frequently expressed in macrophages and can bind multiple ligands including polyanionic substances, extracellular particles, and pathogens. Scavenger receptors are subdivided into eight or nine classes based on sequence

homology and each class is further classified into types. Historically, scavenger receptors of class A, which are expressed on macrophages and have a collagenous structure, were first characterized, and then scavenger receptors of other classes were subsequently identified [30, 31].

In class B scavenger receptors, SR-B1 (SCARB1), CD36 (SR-B2), and LIMP2 (SR-B3, SCARB2) are involved. SR-B1 and the other two receptors have similar structures [32]. A simplified structure of SR-B1 is shown in Fig. 3. Human SR-B1 consisting of 509 amino acids has an extracellular loop, two transmembrane domains, and two intracellular domains. SR-B1 forms oligomers. The N-terminal transmembrane domain, C-terminal region, and cysteine residues in the extracellular loop play an important role in oligomerization. Based on the structural similarity to LIMP2, it is presumed that the extracellular loop forms a tunnel cavity, which facilitates cholesterol transport. The C-terminal intracellular domain contains a binding site to signaling proteins.
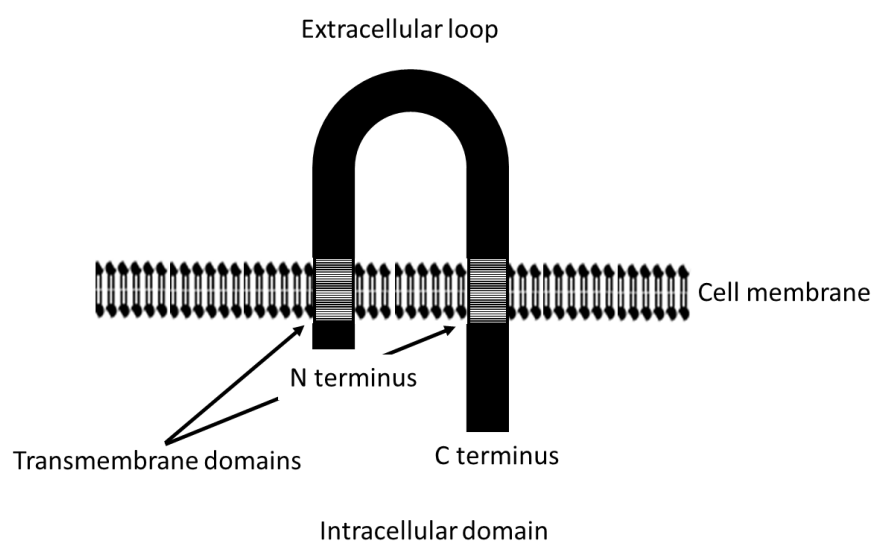

Fig. 3 Simplified structure of SR-B1

SR-B1 functions primarily as a receptor for high-density lipoprotein (HDL). SR-B1 binds to HDL and transports cholesterol into cells from HDL. Although SR-B1 is expressed in a wide variety of cells, hepatocytes and steroidgenic cells of the adrenal gland, testis, and ovary express high levels of SR-B1. Expression of SR-B1 is related to pathogenesis including atherosclerosis, inflammation, hepatitis C virus infection, and cancer. Not only HDL but also various substances can interact with SR-B1, e.g., LDL,

modified LDL, liposomes containing anionic phospholipids such as phosphatidylserine, oxidized phospholipids, modified BSA, apoE, serum amyloid A, silica, endotoxin, and apoptotic cells [33].

When I examined the correlation between endocytosis of liposomes and LD formation in HEK293T cells, I noticed that DOPC/DOPE liposomes are very efficiently endocytosed HEK293T cells, although no correlation was found between the efficacy of liposomal endocytosis and LD formation. Therefore, I investigated the mechanism responsible for the efficient endocytosis of PE-containing liposomes and found that these liposomes are endocytosed into HEK293T cells via SR-B1. I described this study in Chapter III.

1.4. References

1. Bangham, A. D., and R.W. Horne. 1964. Negative staining of phospholipids and their structural modification by surface active agents as observed in the electron microscope. J Mol Biol 8:660-668.

2. Sessa, G, and G. Weissmann. 1968. Phospholipid spherules (liposomes) as a model for biological membranes. J Lipid Res. 9:310-318.

3. Li, J., X. Wang, T. Zhang, C. Wang, Z. Huang, X. Luo, and Y. Deng. 2015. A review on phospholipids and their main applications in drug delivery systems. Asian J Pharm Sci. 10:81-98

4. Alipour, E, D. Halverson, S. McWhirter, and G.C. Walker. 2017. Phospholipid Bilayers: Stability and Encapsulation of Nanoparticles. Annu Rev Phys Chem. 68:261-283.

5. Allen, T. M. and P.R. Cullis. 2013. Liposomal drug delivery systems: from concept to clinical applications. Adv Drug Deliv Rev. 65:36-48.

6. Madni, A., M. Sarfraz, M. Rehman, M. Ahmad, N. Akhtar,   s. Ahmad, N. Tahir, S. Ijaz, R. Al-Kassas, and R. Löbenberg. 2014. Liposomal drug delivery: a versatile platform for challenging clinical applications. J Pharm Pharm Sci. 17:401-426.

7. Abu Lila, A. S. and T. Ishida. 2017. Liposomal delivery systems: design optimization and current applications. Biol. Pharm. Bull. 40:1–10.

8. Zylberberg, C. and S. Matosevic. 2016. Pharmaceutical liposomal drug delivery: a review of new delivery systems and a look at the regulatory landscape. Drug Delivery. 23:3319-3329.

9. Tomori, Y., N. Iijima, S. Hinuma, H. Ishii, K. Takumi, S. Takai, and H. Ozawa. 2018. Morphological Analysis of Trafficking and Processing of Anionic and Cationic Liposomes in Cultured Cells. Acta Histochem Cytochem. 51:81–92.

10. Fadok, V.A., D.L. Bratton, D.M. Rose, A. Pearson, R.A. Ezekewitz, and P.M. Henson. 2000. A receptor for phosphatidylserine-specific clearance of apoptotic cells. Nature. 405:85-90.

11. Zhou, Z. 2007. New phosphatidylserine receptors: clearance of apoptotic cells and more. Dev. Cell. 13:759-760.

12. Armstrong, A.1. and K.S. Ravichandran. 2011. Phosphatidylserine receptors: what is the new RAGE? EMBO Rep. 12:287e288.

13. Bei, Y., S. Das, R.S. Rodosthenous, P. Holvoet, M. Vanhaverbeke, M.C. Monteiro, V.V.S. Monteiro, J. Radosinska, M. Bartekova, F. Jansen, Q. Li, J. Rajasingh, and J. Xiao. 2017. Extracellular Vesicles in Cardiovascular Theranostics. Theranostics. 17:4168-4182.

14. Raposo, G, H.W. Nijman, W. Stoorvogel, R. Liejendekker, C.V. Harding, C.J. Melief, and H.J. Geuze. 1996. B lymphocytes secrete antigen-presenting vesicles. J Exp Med. 183:1161-1172.

15. Hansen, L.L. and M.E. Nielsen. 2017. Plant exosomes: using an unconventional exit to prevent pathogen entry? J Exp Bot. 69:59-68.

16. Toh, W.S., R.C. Lai, B. Zhang, and S.K. Lim. 2018. MSC exosome works through a protein-based mechanism of action. Biochem Soc Trans. 46:843–853.

17. Skotland, T., K. Sandvig, and A. Llorente. 2017. Lipids in exosomes: Current knowledge and the way forward. Prog Lipid Res. 66:30-341.

18. Lin, J., J. Li, B. Huang, J. Liu, X. Chen, X.M. Chen, Y.M. Xu, L.F. Huang, and X.Z. Wang. 2015. Exosomes: Novel Biomarkers for Clinical Diagnosis. Scientific World Journal. 2015:657086.

19. Bunggulawa, E.J., W. Wang, T. Yin, N. Wang, C. Durkan, Y. Wang, and G. Wang. 2018. Recent advancements in the use of exosomes as drug delivery systems. J Nanobiotechnology. 16:81.

20. Li, P., M. Kaslan, S.H. Lee, J. Yao, and Z. Gao. 2017. Progress in Exosome Isolation Techniques. Theranostics 7:789-804.

21. Somiya, M., Y. Yoshioka, and T. Ochiya. 2018. Biocompatibility of highly purified bovine milk-derived extracellular vesicles. J Extracell Vesicles. 7:1440132.

22. Thiam, A.R., R.V.Jr, Farese, and T.C. Walther. 2013. The biophysics and cell biology of lipid droplets. Nat Rev Mol Cell Biol. 14:775-786.

23. Welte, M.A. and A.P. Gould. 2017. Lipid droplet functions beyond energy storage. Biochim Biophys Acta. 1862:1260-1272.

24. Sztalryda, C. and D.L. Brasaemleb. 2017. The perilipin family of lipid droplet proteins: Gatekeepers of intracellular lipolysis. Biochim Biophys Acta. 1862:1221-1232.

25. Olzmann, J.A. and P. Carvalho. 2019. Dynamics and functions of lipid droplets. Nature Reviews Mol. Cell Biol. 20:138-155.

26. Nishikawa, K., H. Arai, and K. Inoue. 1990. Scavenger receptor-mediated uptake and metabolism of lipid vesicles containing acidic phospholipids by mouse peritoneal macrophages. J. Biol. Chem. 265:5226-531.

27. Namatame, I., H. Tomoda, H. Arai, K. Inoue, and S. Omura. 1999. Complete inhibition of mouse macrophage-derived foam cell formation by triacsin C. J. Biochem. 125:319-327.

28. Amano, C., H. Minematsu, K. Fujita, S. Iwashita, M. Adachi, K. Igarashi, and S. Hinuma. 2015. Nanoparticles Containing Curcumin Useful for Suppressing Macrophages In Vivo in Mice. PLoS One. 10:e0137207.

29. Fujita, K., Y. Hiramatsu, H. Minematsu, M. Somiya, S. Kuroda, M. Seno, and S. Hinuma. 2016. Release of siRNA from Liposomes Induced by Curcumin. Journal of Nanotechnology 2016: Article ID 7051523.

30. Canton1, J., Neculai, D., Grinstein, S. 2013. Scavenger receptors in homeostasis and immunity. Nature Reviews Immunology 13: 621-634.

31. PrabhuDas, M., Bowdish, D., Drickamer, K., Febbraio, M., Herz, J., Kobzik, L., Krieger, M., Loike, J., Means, T. K., Moestrup, S. K., Post, S., Sawamura, T., Silverstein, S., Wang,X-Y., Khoury, J. E. 2014. Standardizing scavenger receptor nomenclature. 192: 1997–2006.

32. Neculai, D., Schwake, M., Ravichandran, M., Zunke, F., Collins, R. F., Peters, J,

Neculai, M., Plumb, J., Loppnau, P., Pizarro, J. C., Seitova, A., Trimble, W. S., Saftig, P., Grinstein, S., Dhe-Paganon, S.. 2013. Structure of LIMP-2 provides functional insights with implications for SR-BI and CD36. Nature. 504:172-6.

Chapter II

Induction of lipid droplets in non-macrophage cells as well as macrophages by liposomes and exosomes

2.1. Abstract

It has been reported that phospholipid nanoparticles (PNPs) including liposomes and exosomes could efficiently induce lipid droplets (LDs) in macrophages. However, in non-macrophage cells, the effects of PNPs on the induction of LDs have not been thoroughly investigated. In this report, we directly compared non-macrophage and macrophage cell lines in terms of LD induction by various formulation of liposomes containing phosphatidylserine and exosomes. All non-macrophage cell lines as well as macrophage cell lines tested in this study showed evident LD induction in response to these PNPs. Though the efficacy of LD induction in non-macrophage cell lines varied considerably, the results in this study suggest that LD formation is a common and crucial response to PNPs in mammalian cells not only in macrophages but also in nonmacrophage cells.

2.2. Introduction

Artificial nanoparticles prepared using phospholipids have been referred to as liposomes [1,2]. They have been frequently used as carriers in drug delivery systems (DDSs) because they could contain a variety of substances. In fact, some medical drugs utilizing liposomes as carriers have already been launched [3]. Therefore, the carrier functions of liposomes in DDSs have been a subject of interest, whereas the biological effects of liposomes by themselves on cells might not have been studied thoroughly. Recent studies demonstrate that there are naturally occurring phospholipid particles (i.e., extracellular vesicles) in body fluids. Nano-sized extracellular vesicles are referred to as exosomes [4,5]. Exosomes are released from cells and are thought to play important roles in cell-to-cell communication by delivering bioactive substances. Since both liposomes and exosomes are phospholipid nanoparticles (PNPs), liposomes can be regarded as a

simple model of exosomes. Lipid droplets (LDs) are an intracellular organelle existing in most mammalian cells [6,7]. They mainly contain triacylglycerol and cholesteryl ester, surrounded by a monolayer of phospholipids, in which various specific proteins are integrated. An important function of LDs has been thought to be energy storage that is utilized in a nutrient deficient environment [8]. However, recent studies suggest that LDs have divergent functions beyond energy storage [7]. It has been reported that liposomes and exosomes could induce LDs in macrophages [9-11]. However, it has not been clarified in detail whether PNPs can efficiently induce LDs even in non-macrophage cells, and few reports are available that directly compare LD formation induced by PNPs in non-macrophage cells and macrophages. In this report, I demonstrate that both liposomes and exosomes could efficiently induce LDs in nonmacrophage as well as macrophage cell lines.

2.3. Materials and methods

2.3.1. Preparation of liposomes

I prepared liposomes according to the methods described previously [12,13]. The phospholipids, 1,2-dioleoyl-sn-phosphatidylcholine (DOPC), 1,2-dioleoyl-sn-phosphatidylethanolamine (DOPE), 1,2-dioleoyl-sn-glycero-3-phospho-Lserine (DOPS) and 1,2-dipalmitoyl-sn-glycero-3-phosphocholine (DPPC) were purchased from the NOF corporation, and 1,2-dioleoyl-3-trimethylammonium-propane (DOTAP) was purchased from Avanti. Egg yolk-derived lecithin was obtained from Nacalai Tesque. Cholesterol was purchased from Sigma-Aldrich. Briefly, 12 mg of a mixture of phospholipids was dissolved in chloroform (4 mL), and then the solution was evaporated in an eggplant-shaped flask. After 4mL of phosphate-buffered saline (PBS) was added to the flask, it was vortexed. If necessary, the obtained suspension was sonicated, and then extruded using a 100-nm pore-size membrane. The liposomal suspensions thereby obtained were dialyzed against PBS using a Spectra/Por CE dialysis tube (cut off molecular weight of 1,000KD; Repligen Co.). The resultant suspension was filtered through a 0.22-mm membrane (Millipore). Polystyrene beads (surface unmodified) were purchased from Micromod Partikeltechnologie.

2.3.2. Preparation of exosomes

Exosomes were prepared from defatted bovine milk (Koiwai defatted milk, Japan) by the method reported previously [14]. Briefly, defatted milk was mixed with acetic acid, and then centrifuged at 1×10^4 g for 10 min at 4 °C. After resultant supernatants were filtered with a 0.22-mm membrane, they were subjected to ultracentrifugation using a himac CP 100MX (Hitachi) equipped with a rotor PS40ST at 1.49×10^5 g for 70 min at 4 °C. Supernatants were discarded, and exosome-containing pellets were collected. After washing once with PBS by ultracentrifugation at 1.49×10^5 g for 70 min at 4 °C, the pellets were resuspended in PBS. Aggregates in the suspension were separated via centrifugation at 1×10^4 g for 5 min at 4 °C. The resultant suspension was filtered using a 0.22-mm membrane.

2.3.3. Physicochemical analyses of nanoparticles

Particle sizes and polydispersity indexes (PDIs) of PNPs were measured using the Zetasizer Nano ZS (Malvern) based on dynamic light scattering, while zeta-potentials were determined using electrophoretic light scattering. I quantified the total lipid and phospholipid contents of PNPs by sulfo-phospho-vanillin and the Stewart method, respectively [15,16]. To estimate the total lipids and phospholipids of exosomes, I extracted lipids from exosomes using chloroform, and then I measured by sulfo-phospho-vanillin and the Stewart method, respectively. I used DPPC/lecithin (a weight ratio of 1:1) liposomes as a standard for quantifying the total lipids of exosomes, because I assumed here that exosomes contain equal amounts of saturated and unsaturated lipids. Protein concentrations were determined using the Lowry method; bovine serum albumin was used as a standard.

2.3.4. Cell culture

HEK293T, THP-1, L929, RAW264.7, COS-7, Neuro-2a, and HuH-7 were obtained from RIKEN RBC. These cells were principally maintained in RPMI1640 medium (Gibco) supplemented with antibiotics (penicillin and streptomycin; Gibco) and 10% heat-inactivated fetal calf serum (FCS; Biowest) in tissue culture flasks (Corning) or dishes (Nunc). To examine the effects of PNPs on LD induction in cultured cells, I diluted

PNP suspensions with PBS, and then admixed them with an equal volume of a cell suspension (4×10^5/mL) in the RPMI1640 medium (Gibco) containing 10% heat-inactivated FCS. Cells (final concentration of 2×10^5/mL) were cultured in the presence or absence of PNPs in 5% CO_2 at 37 °C for 24 h. To examine THP-1 cells activated by phorbol 12-myristate 13- acetate (PMA, Sigma-Aldrich), I incubated these cells with 100 nM of PMA for 24 h before adding PNPs.

2.3.5. Fluorescence-labeled liposomes and exosomes.

To track the location of liposomes or exosomes in HEK293T cells by fluorescence microscopy, I labeled these PNPs with a fluorescent reagent (0.1 mg/mL), CellTracker CM-Dil (Thermo Fisher Scientific), according to the manufacturer's instructions.

2.3.5. Fluorescence microscopy

To prepare cells for subjecting to fluorescence microscopy, I pre-cultured HEK293T cells in RPMI1640 medium containing 10% FCS (2×10^4/mL, 200 mL/well) using an 8-well chambered cover glass (Thermo Fisher Scientific) that was pre-coated with poly-L-lysine for 24 h allowing the cells to firmly adhere to the cover glass. The medium was then changed to a fresh test medium (400 mL) containing equal volumes of RPMI1640 medium containing 10% FCS and a PNP suspension in PBS. After culturing for 24 h, adherent cells were washed once with PBS, and then fixed with 100 mL/well of 4% (w/v) paraformaldehyde in PBS containing Hoechst33342 (Thermo Fisher Scientific) for 10 min at room temperature. The fixed cells were washed once with PBS, and subsequently stained with 0.4 mg/mL of Nile red (Wako) or 5 mg/mL of BODIPY 493/503 (Sigma-Aldrich) in PBS (200 mL) for 30 min at room temperature [17,18]. After these cells were washed once with PBS, they were mounted with Fluoro-KEEPER antifade reagent (Nacalai Tesque). Cells were observed under a confocal laser scanning microscope FV-1000 (Olympus) at room temperature as described before [19]. The microscope was equipped with a UPlanSApo lens (oil, × 100, and NA ¼ 1.40) (Olympus). Images were analyzed and constructed using the software FV10-AWS ver. 4.2a (Olympus).

2.3.6. Flow cytometric analyses

Cells were cultured in the test medium (2 mL/well) with or without PNPs in a 12-well tissue culture microplate (Corning). All cells were washed once with PBS, and then harvested from the plate by trypsinization (in the case of adherent cells). The cell suspension was centrifuged in a tube at 1500 rpm for 5 min at 4 °C and washed once with PBS. To detect LDs in cells, live cells were stained with 200 mL of Nile red solution (0.4 mg/mL in PBS) at 4 °C for 30 min according to a previously described method [17]. In each specimen, the fluorescence of 1.0×10^4 cells was analyzed using a FACSCant II (BD Biosciences). The intensity of intracellular fluorescence in each specimen was measured as a geometric mean. Relative fluorescence intensity was calculated by the following formula: (A-C)/(B-C); A: geometric mean of fluorescence intensity in PNP-treated cells after Nile red staining, B: geometric mean of fluorescence intensity in untreated cells after Nile red staining and C: geometric mean of fluorescence intensity of untreated cells without staining. Relative fluorescence values were expressed as mean ± SD (n = 3, vertical bars). Statistical analyses of data were performed by the Student's t-test (*: $p < 0.05$ and **: $p < 0.01$, vs. control).

2.3.7. Transmission electron microscopy (TEM)

COS-7 cells (5×10^4/mL) were cultured on a Cell Desk (Sumitomo Bakelite Co., Ltd.) in the test medium (1 mL) for 72 h in the presence of DOPC/DOPE liposomes (250 mg/mL). The cells were then fixed with 2% formaldehyde and 2.5% glutaraldehyde in 0.1M phosphate buffer (pH 7.4) and washed thrice for 5 min with 0.1M phosphate buffer (pH 7.4) containing 4% sucrose. The cells were post-fixed for 1 h with 1% osmium tetroxide and 0.5% potassium ferrocyanide in 0.1M phosphate buffer (pH 7.4), and then dehydrated with a graded series of ethanol (50, 70, 90, and 100% ethanol). For staining the LDs in the cell, 1% p-phenylenediamine was added to 70% ethanol during dehydration. The samples were embedded in Epon812 (TAAB Co. Ltd.) and 80-nm ultra-thin sections were stained with saturated uranyl acetate and lead citrate solution. Electron micrographs were obtained with a JEM-1400plus transmission electron microscope.

2.3.8. Treatment with metabolic inhibitors

In experiments to test the effect of lipid metabolic inhibitors, I used pyrrolidine-2 (phospholipase A2 inhibitor; Merck), etomoxir sodium (carnitine palmitoyltranseferase-1 inhibitor; Sigma-Aldrich), and triacsin C (acyl-CoA synthetase inhibitor; Enzo Life Sciences). Cells were pre-cultured with these inhibitors for 4 h, respectively, and then DOPC/DOPE liposomes were added to the culture. After culture for 24 h with or without liposomes, LDs in cells were quantified using flow cytometer.

2.4. Results

2.4.1. Preparation of nanoparticles used to induce LDs

It has been reported that liposomes containing phosphatidylserine and those consisting of unsaturated acyl groups have abilities to efficiently induce LDs in peritoneal macrophages and a macrophage cell line [9,10]. I therefore prepared liposomes constituted with various kinds of phospholipids including phosphatidylserine to examine their LD-inducing activities on non-macrophage cell lines as well as macrophage cell lines. As shown in Table 1, I prepared approximately 100-nm size of liposomes (range of 76.7-215 nm). To prepare these liposomes, I performed dialysis of their suspensions against PBS after extruder treatment, because PDIs of DOPC/DOPS liposomes were over 0.5 without dialysis, whereas their PDIs were improved to less than 0.3 after dialysis. Though the recovery of DOPC/DOPS liposomes was substantially reduced by this procedure. I obtained exosomes from defatted milk as described previously [14]. I confirmed that my preparation of exosomes contained some amounts of phospholipids, though it should be noted that the estimated amounts of total lipids and phospholipids in exosomes were relative values against the standard because the estimation of lipid amounts in exosomes varied depending on a standard sample used to make a calibration curve in the colorimetric assay.

2.4.2. Induction of lipid droplets in HEK293T cells by DOPC/DOPS liposomes and exosomes

HEK293T is a non-macrophage cell line obtained from HEK293 cells by introducing SV40T antigen. Origin of HEK293 cells has been suggested to be neuronal cells contained in human embryonic kidney cells [20]. I found that LDs were efficiently induced in HEK293T cells in response to PNPs. As shown in Fig. 1, in HEK293T cells cultured without PNPs (Fig. 1A), LDs were rarely detectable by Nile red staining [17]. In contrast, after treatment of these cells with DOPC/DOPS liposomes (Fig. 1B) or exosomes (Fig. 1C) for 24 h, abundant LDs appeared in cells. To confirm the uptake of PNPs in HEK293T cells, I prepared fluorescence-labeled PNPs, and then examined the intracellular distributions of the labeled PNPs and LDs after treatment of these cells with PNPs. In HEK293T cells cultured in the absence of the fluorescence-labeled PNPs (Fig. 1D), the fluorescence of these particles was not detected in the cells, whereas in the cells treated with the labeled liposomes (Fig. 1E) or exosomes (Fig. 1F), their fluorescence was detected in the cytoplasm respectively. In these experiments (Fig. 1DeF), I stained LDs by BODIPY 493/503 which is also used to detect intracellular LDs [18]. Fig. 1G-I shows phase-contrast microscopic images overlaid with fluorescent images of Fig. 1 to F, respectively. These data indicate that almost all LDs and PNPs are distributed in the cytoplasm rather than on the cell membrane. Furthermore, the distribution of LDs apparently differed from that of the labeled PNPs, which suggests that PNPs incorporated into cells were not directly delivered into LDs. My data does not rule out the possibility that a part of PNP components are delivered to LDs, because it has been reported that fatty acids of liposomes are transferred to LDs [9].

2.4.3. LD-inducing activities of various nanoparticles to HEK293T and COS-7 cells

I examined LD-inducing activities of various nanoparticles including liposomes, exosomes and polystyrene beads have on HEK293T cells (Fig. 2A). LD-inducing activities of liposomes varied considerably depending on their constituents of phospholipids. In my preparation of liposomes, DOPC/DOPS liposomes exhibited the highest activity, whereas the activity of DOPC/DOPE liposomes, which did not contain DOPS, was estimated to be one-fortieth less than that of DOPC/DOPS (i.e., LD induction of DOPC/DOPS liposomes at 6.3 mg/mL was greater than that of DOPC/DOPE

liposomes at 6.3 mg/mL). It has been reported that liposomes containing phosphatidylserine exhibit high LD-inducing activities on peritoneal macrophages and a macrophage cell line [9]. My results are consistent with those of the previous report. However, in my study, DOPC/DOPS liposomes show high LD-inducing activities not only in macrophage cell lines but also in non-macrophage cell lines. On the other hand, liposomes containing cholesterol showed one-twentieth lower LD-inducing activities than DOPC/DOPS liposomes (i.e., LD induction of DOPC/DOPS liposomes at 12.5 mg/mL was greater than those of DOPC/DOPS/Cholesterol and DOPC/DOPE/DOPS/Cholesterol liposomes at 250 mg/mL), which indicates that cholesterol does not enhance LD-inducing activities as a phosphatidylserine. Interestingly, cationic liposomes (DOPC/DOTAP liposomes) also showed high LD-inducing activity. These results suggest that the negative charge of liposomes is not essential for LD-inducing activities. Polystyrene beads, which have a comparable negative charge to DOPC/DOPS liposomes, did not show LD induction in HEK293T cells, which suggests that LD inducing activities are a property closely associated with PNPs. Exosomes as well as DOPC/DOPS liposomes evidently promoted LD formation in HEK293T cells. In an African green monkey fibroblastic cell line, COS-7 cells, PNPs exhibited the induction of LDs in a similar manner to HEK293T cells (Fig. 2B). To confirm the intracellular distribution of LDs precisely, I analyzed LDs in COS-7 cells induced by DOPC/DOPE liposomes by TEM. As shown in Fig. 2C, abundant LDs with low electric density were detected in the cytoplasm of COS-7 cells.

2.4.4. Induction of LDs in a variety of cell lines by DOPC/DOPS liposomes and exosomes

After treatment with DOPC/DOPS liposomes and exosomes, I examined LD induction in non-macrophage as well as macrophage cell lines (Fig. 3). Non-macrophage cell lines used here were HEK293T, L929 (a mouse fibroblastic cell line), COS-7, Nuero2a (a mouse neuroblastoma cell line) and HuH7 (a human liver carcinoma cell line), while THP-1 (a human monocytic leukemia cell line) and RAW264.7 (a mouse macrophage cell line) were used as macrophage cell lines. I also used THP-1 cells treated with PMA to obtain differentiated and activated status of macrophages. DOPC/DOPS liposomes could induce LDs in non-macrophage cell lines as well as macrophage cell lines, though LD induction was relatively low in Neuro2a and HuH7. I could not analyze the LD-

inducing activity of DOPC/DOPS liposomes in THP-1 cells, because almost all of these cells died in culture with 25 mg/mL of DOPC/DOPS liposomes. I therefore compared LD-inducing activities by treatment with lower doses of DOPC/DOPS liposomes between THP-1 and HEK293T cells, and I found that THP-1 cells showed a LD induction level comparable to HEK293T cells (data not shown). Under my experimental conditions, PMA treatment of THP-1 cells merely induced a slight enhancement of LD induction. Similar results were obtained by the treatment of exosomes. Exosomes induced LDs in non-macrophage as well as macrophage cell lines. As shown in Fig. 3C, a correlation of LD inductions (R2 = 0.499) between treatment with DOPC/DOPS liposomes and exosomes were observed. It was suggested that common mechanisms worked to promote LD formation between the two PNPs.

2.4.5. Suppression of LDs induction by inhibitors of lipid metabolism

I examined the effect of inhibitors against lipid metabolism, i.e., pyrrolidine-2 (phospholipase A2 inhibitor), etomoxir (carnitine palmitoyltranseferase-1 inhibitor), and triacsin C (acyl-CoA synthetase inhibitor), on LD formation in COS-7 cells induced by liposomes. The dose of inhibitors used was effective in suppressing LD formation as previously reported [8, 23]. The LD content was assessed by flow cytometry after NR staining. As shown in Fig. 4, the LD content was increased after liposomal treatment in the absence of inhibitors after 24 h. Neither Pyrrolidine-2 nor Etomoxir influenced the LD content of cells in the absence of liposomes. Although change in LD induction was detected at 30 µM of etomoxir after treatment with liposomes, this reduction was marginal. On the other hand, triacsin C at doses of 2 and 10 µM drastically reduced LD formation induced by liposomal treatment in a dose-dependent manner; however, triacsin C reduced LD formation in the absence of liposomes.

2.5. Discussion

In this study, I demonstrated that DOPC/DOPS liposomes and exosomes could induce LDs in non-macrophage cell lines as well as macrophage cell lines. It has been reported that liposomes, which are composed of phosphatidycholine, phosphatidylserine,

cholesterol, diacetylphosphate and 1,2-di[1-14C]palmitoyl-glycerophosphocholine with a molar ratio of 50:50:75:10:0.5, efficiently induced neutral lipids in peritoneal macrophages and a macrophage cell line, whereas these liposomes failed to induce neutral lipids in a fibroblastic cell line [9]. However, in my study, DOPC/DOPS liposomes apparently induced LDs in non-macrophage cell lines including fibroblastic cell lines. The apparent difference in the results could be explained by following reasons: (1) DOPC/DOPS liposomes containing 50% of DOPS employed in my study are expected to have greater LD-inducing activity than liposomes containing 26% of bovine brain-derived phosphatidylserine used in the previous report; (2) I directly quantified LDs in cells by flow cytometric analyses, whereas LDs were indirectly estimated through neutral lipids in the previous report; (3) even in my data, responsibilities of non-macrophage cell lines to DOPC/DOPS liposomes substantially varied, so that my results do not deny the existence of low-responsive cell lines in terms of LD induction. My preliminary data indicated that in response to DOPC/DOPS liposomes and exosomes, HEK293T cells exhibited efficient LD induction as macrophages prepared from mice (data not shown).

My data suggests that LD induction is a common response to PNPs in mammalian cells not only macrophages but also non-macrophage cells. In this study, I demonstrated that various PNPs could induce LDs in HEK293T cells. However, the interaction of these PNPs and the cell membrane of HEK293T would not necessarily be identical. For instance, cationic liposomes interact with cultured cell membrane quite differently from anionic liposomes [21]. In addition, phosphatidylserine receptors have been extensively investigated, and multiple molecules have been reported to function as phosphatidylserine receptors [22]. It is therefore considered that even if the interaction between each PNP and cell membrane is not always identical among PNPs, there is a common signaling or metabolic pathway(s) which result in enhance LD formation.

In this study, the acyl-CoA synthetase inhibitor, which inhibits TAG synthesis, completely negated the increase in LD formation induced by liposomes. These results were consistent with the previous report that LD formation in macrophages induced by liposomes containing phosphatidylserine is inhibited by the acyl-CoA synthetase inhibitor [23]. Therefore, acyl-CoA synthetase plays a crucial role in the process of LD formation induced by liposomes. Future study is necessary to clarify more precise mechanisms responsible for PNP-induced LD induction observed widely in mammalian cells.

2.6. References

1. Bangham, A.D., and R.W. Horne. 1964. Negative staining of phospholipids and their structural modification by surface active agents as observed in the electron microscope. J. Mol. Biol. 8:660-668.

2. Sessa, G., and G. Weissmann. 1968. Phospholipid spherules (liposomes) as a model for biological membranes. J. Lipid Res. 9:310-318.

3. Alipour, E., D. Halverson, S. McWhirter, and G.C. Walker. 2017. Phospholipid bilayers: stability and encapsulation of nanoparticles. Annu. Rev. Phys. Chem. 68:261-283.

4. Raposo, G., H.W. Nijman, W. Stoorvogel, R. Liejendekker, C.V. Harding, C.J. Melief, and H.J. Geuze. 1996. B lymphocytes secrete antigen-presenting vesicles. J. Exp. Med. 183:1161-1172.

5. Bei, Y., S. Das, R.S. Rodosthenous, P. Holvoet, M. Vanhaverbeke, M.C. Monteiro, V.V.S. Monteiro, J. Radosinska, M. Bartekova, F. Jansen, Q. Li, J. Rajasingh, and J. Xiao. 2017. Extracellular vesicles in cardiovascular theranostics. J. Theranostics. 7:4168-4182.

6. Thiam, A.R., R.V. Farese Jr., and T.C. Walther. 2013. The biophysics and cell biology of lipid droplets. Nat. Rev. Mol. Cell Biol. 14:775-786.

7. Welte, M.A. and A.P. Gould. 2017. Lipid droplet functions beyond energy storage. Biochim. Biophys. Acta 1862:1260-1272.

8. Cabodevilla, A.G., L. Sanchez-Caballero, E. Nintou, V.G. Boiadjieva, F. Picatoste, A. Gubern, and E. Claro. 2013. Cell survival during complete nutrient deprivation depends on lipid droplet-fueled b-oxidation of fatty acids. J. Biol. Chem. 288:27777-27788.

9. Nishikawa, K., H. Arai, and K. Inoue. 1990. Scavenger receptor-mediated uptake and metabolism of lipid vesicles containing acidic phospholipids by mouse peritoneal macrophages. J. Biol. Chem. 265:5226-5231.

10. Fujiwara, Y., K. Hama, M. Tsukahara, R. Izumi-Tsuzuki, T. Nagai, M. Ohe-Yamada, K. Inoue, and K. Yokoyama. 2018. Acyl chain preference in foam cell formation from mouse peritoneal macrophages. Biol. Pharm. Bull. 41:86-91.

11. Zakharova, L., M. Svetlova, and A.F. Fomina. 2007. T cell exosomes induce cholesterol accumulation in human monocytes via phosphatidylserine receptor. J. Cell. Physiol. 212:174-181.

12. Amano, C., H. Minematsu, K. Fujita, S. Iwashita, M. Adachi, K. Igarashi, and S. Hinuma. 2015. Nanoparticles containing curcumin useful for suppressing macrophages in vivo in mice. PLoS One 10:e0137207.

13. Fujita, K. H. Yoshie, H. Minematsu, M. Somiya, S. Kuroda, M. Seno, and S. Hinuma. 2016. Release of siRNA from liposomes induced by curcumin. Journal of Nanotechnology 2016:7051523, https://doi.org/10.1155/2016/7051523, 6 pages.

14. Somiya, M. Y. Yoshioka, and T. Ochiya. 2018. Biocompatibility of highly purified bovine milk-derived extracellular vesicles. J. Extracell. Vesicles 7:1440132.

15. Frings, C.S., T.W. Fendley, R.T. Dunn, and C.A. Queen. 1972. Improved determination of total serum lipids by the sulfo-phospho-vanillin reaction. Clin. Chem. 18:673-674.

16. Stewart, J.C. 1980. Colorimetric determination of phospholipids with ammonium ferrothiocyanate. Anal. Biochem. 104:10-14.

17. Greenspan, P. E.P. Mayer, and S.D. Fowler. 1985. Nile red: a selective fluorescent stain forintracellular lipid droplets. J. Cell Biol. 100:965-973.

18. Qiu, B. and M.C. Simon. 2016. BODIPY 493/503 staining of neutral lipid droplets formicroscopy and quantification by flow cytometry. Bio Protoc 6:e1912.

19. Somiya, M., Q. Liu, N. Yoshimoto, M. Iijima, K. Tatematsu, T. Nakai, T. Okajima, K. Kuroki, K. Ueda, and S. Kuroda. 2016. Cellular uptake of hepatitis B virus envelope L particles is independent of sodium taurocholate cotransporting polypeptide, but dependent on heparan sulfate proteoglycan. Virology 497:23e32.

20. Shaw, G., S. Morse, M. Ararat, and F.L. Graham. 2002. Preferential transformation of human neuronal cells by human adenoviruses and the origin of HEK 293 cells. FASEB J. 16:869e871.

21. Tomori, Y., N. Iijima, S. Hinuma, H. Ishii, K. Takumi, S. Takai, and H. Ozawa. 2018. Morphological analysis of trafficking and processing of anionic and cationic liposomes in cultured cells. Acta Histochem. Cytoc. 51:81e92. doi:10.1267/ahc.17021.

22. Armstrong, A. and K.S. Ravichandran. 2011. Phosphatidylserine receptors: what is the new RAGE? EMBO Rep. 12:287-288.

23. Namatame I., H. Tomoda, H. Arai, K. Inoue, and S. Omura. 1999. Complete inhibition of mouse macrophage-derived foam cell formation by triacsin C. J Biochem. 125:319-327.

Table 1 Properties of nanoparticles used in this study.

Nanoparticle	Size (nm) ‡ [PDI]	Zeta-potential§	Total lipid (mg/mL) ∥ [Recovery (%)] ¶	Phospholipid (mg/mL) ††	Protein (mg/mL) [Recovery (mg/L)] ‡‡
DOPC/DOPE liposomes†	111.5±18.5 [0.17±0.07] N = 19	-13.8±7.4 N = 19	4.45±0.91 [84.7±15.3] N =19	N.D.	N.D.
DOPC/DOPS liposomes†	127.3±32.4 [0.31±0.14] N = 5	-55.9±7.8 N = 5	0.94±0.32 [27.3±14.0] N = 5	N.D.	N.D.
DOPC/DOTAP liposomes†	76.7 [0.23] N =1	+34.9 N = 1	2.30 [53.7] N = 1	N.D.	N.D.
DOPC/DOPE/ DOPS/Cholesterol liposomes†	215.0 [0.22] N = 1	-36.7 N = 1	2.77 [53.7] N = 1	1.47 N = 1	N.D.
DOPC/DOPS/ Cholesterol liposomes†	122.5 [0.17] N = 1	-29.8 N = 1	2.53 [45.8] N = 1	2.03 N = 1	N.D.
Exosomes	155.5±11.1 [0.16±0.17] N = 5	-17.7±0.6 N = 5	0.39±0.09 N = 3	0.19±0.002 N = 3	1.21±0.35 N = 5 [6.7±2.8]
Polystyrene beads	109.5 [0.01] N = 1	-50.8 N = 1	N.D.	N.D.	N.D.

† : molar ratios of lipid compositions, DOPC:DOPE = 10:11; DOPC:DOPS = 10:10; DOPC : DOTAP = 10:11; DOPC : DOPS : Cholesterol = 10:2:12; DOPC : DOPE : DOPS : Cholesterol =10:11:3:20. ‡: the amounts of total lipid in liposomes were determined using the sulfo-phospho-vanillin method, while those of exosomes were estimated from a calibration curve obtained using DPPC/lecithin (molar ratio of 1:1) liposomes. §: recovery of liposomes was expressed as the percentage (w/w) of liposomes to lipids

dissolved initially in the solvent. Liposomal suspensions prepared were approximately 2.6 mL. ||: phospholipids were quantified using the Stewart method (absorbance at 488 nm) and a calibration curve was obtained using DPPC/lecithin liposomes. ¶: recovery of exosomes was expressed as the protein weight of exosomes to 1 L of defatted milk. Exosomal suspensions obtained from 1 L of defatted milk were approximately 5.3 mL. Values were expressed mean ± SD. N: number of samples tested. N.D.: not determined.
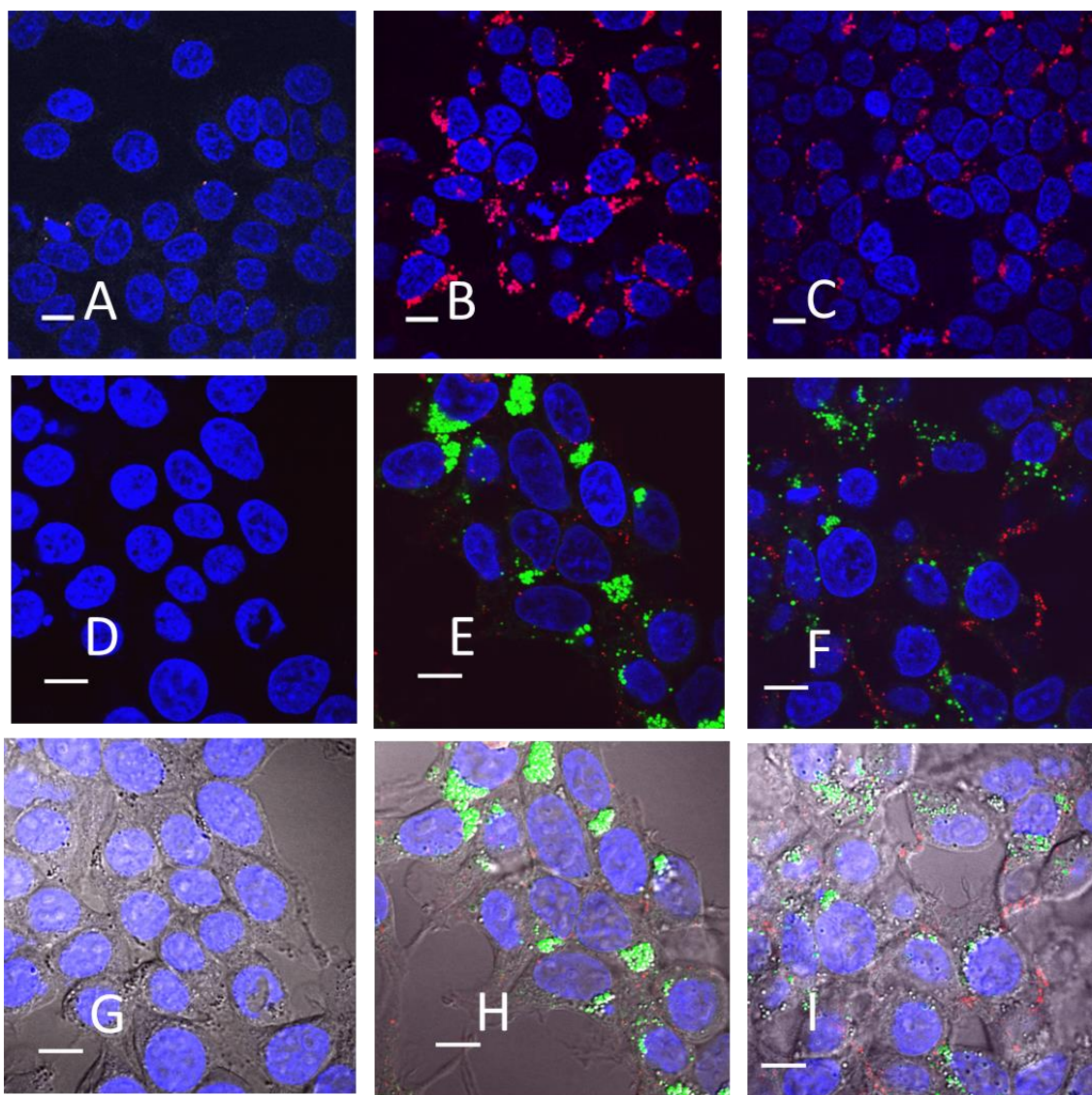
Fig. 1. Induction of LDs in HEK293T cells by treatment with DOPC/DOPS liposomes and exosomes. HEK293T cells were treated with DOPC/DOPS liposomes (25 mg/mL) or exosomes (250 mg/mL), respectively. After cells were fixed and stained, they were subjected to fluorescence microscopy. A: untreated control; B: treated with DOPC/DOPS liposomes; C: treated with exosomes. A to C: nuclei and LDs were stained using Hoechst 33342 (blue) and Nile red (red), respectively. D: untreated control; E: treated with CM-Dil-labeled DOPC/DOPS liposomes (red); F: treated with CM-Dil-labeled exosomes (red). D to F: nuclei and LDs were stained using Hoechst 33342 (blue) and BODIPY 493/503 (green), respectively. G to I: phase-contrast images were overlaid with fluorescent images of D to F, respectively. Bars in images indicate 10 mm. (For interpretation of the references to color in this figure legend, the reader is referred to the Web version of this article.)
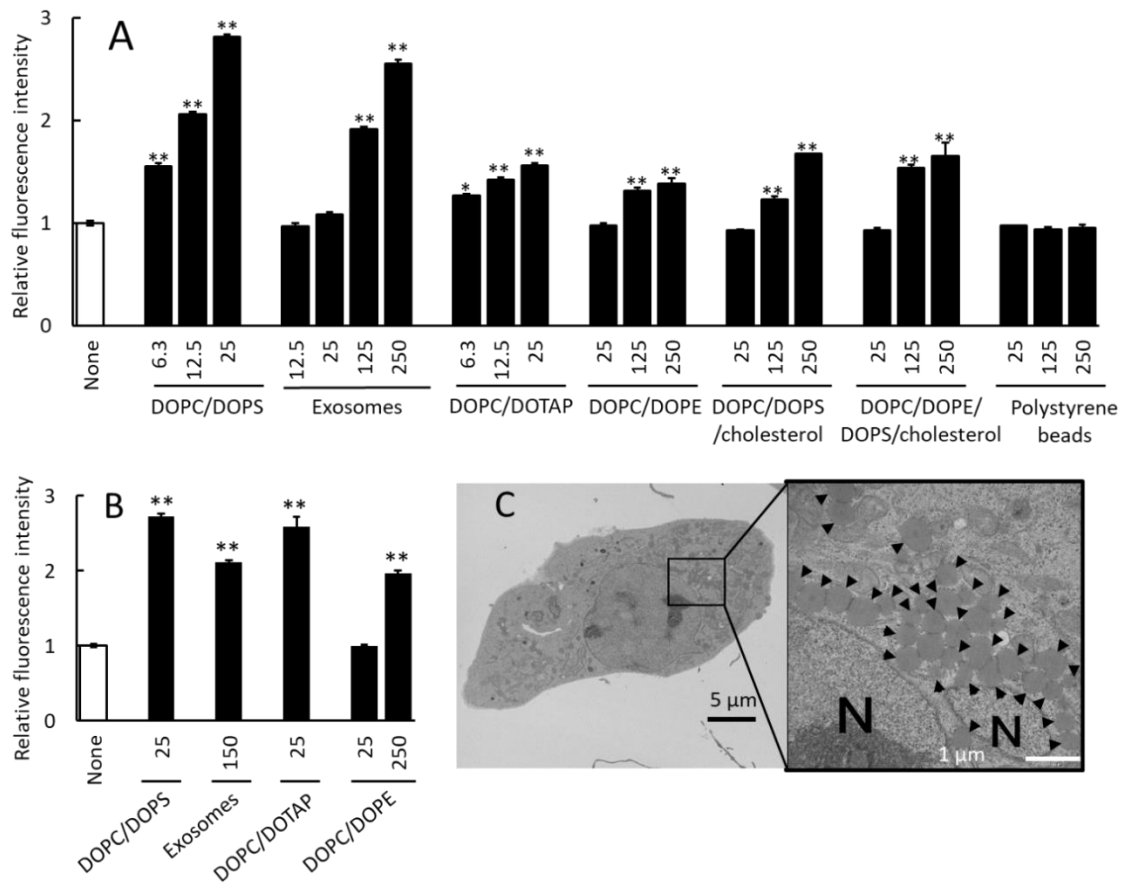
Fig. 2. Effect of various nanoparticles on LD induction in HEK293T or COS-7 cells. HEK293T cells (A) or COS-7 cells (B) were cultured for 24 h or 72 h respectively, and then they were subjected to flow cytometry. Fluorescence intensity of cells cultured without nanoparticles (control, an open column) was defined as 1.0, and each value of fluorescence in cells treated with nanoparticles (closed columns) was expressed as a relative fluorescence intensity to the control value. Doses of nanoparticles were indicated as numeric values under the columns. Note that doses of liposomes, exosomes and polystyrene beads were based on total lipid, protein and polystyrene (mg/ml), respectively. C: TEM image of LDs in DOPC/DOPE liposome-treated COS-7 cells at low (left) and high (right) magnification, respectively. Arrows and N indicate lipid droplets and nucleus, respectively. Scales are indicated as bars.
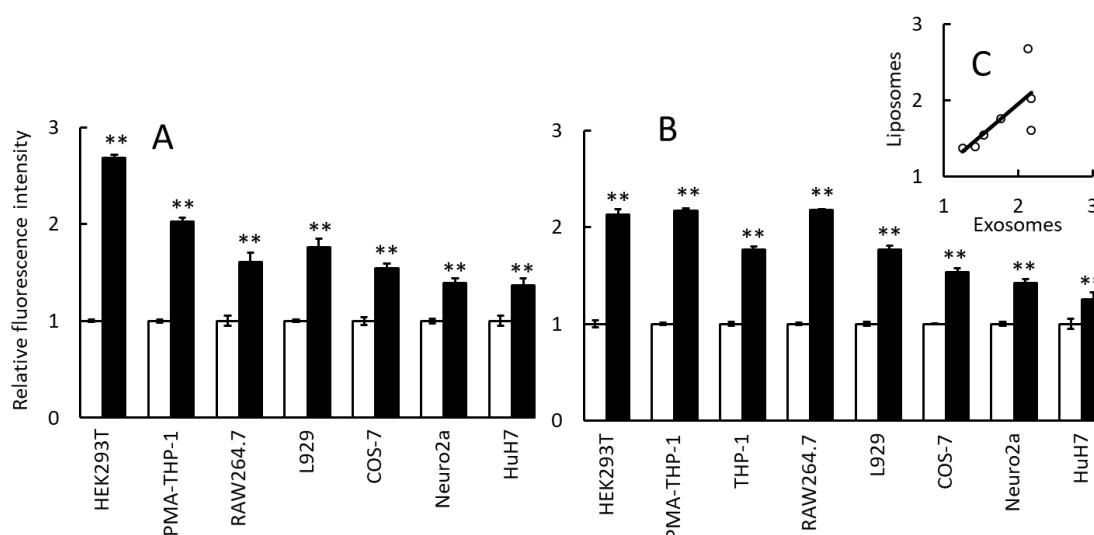
Fig. 3. Induction of LDs in non-macrophage as well as macrophage cell lines by DOPC/DOPS liposomes and exosomes. Indicated cell lines were cultured in the presence or absence of DOPC/DOPS liposomes (25 mg/mL of total lipid, panel A) or exosomes (150 mg/mL of protein, panel B) for 24 h, respectively. After the culture, cells were stained with Nile red and analyzed by flow cytometry. Fluorescence intensity of cells cultured without nanoparticles (control, an open column) was defined as 1.0, and each fluorescence value in cells treated with nanoparticles (closed columns) was expressed as a ratio (relative fluorescence intensity) to the control value. C: a correlation chart on which the relative fluorescence intensities of liposome- and each exosome-treated cell line were plotted as a circle; a regression line is shown on the chart.
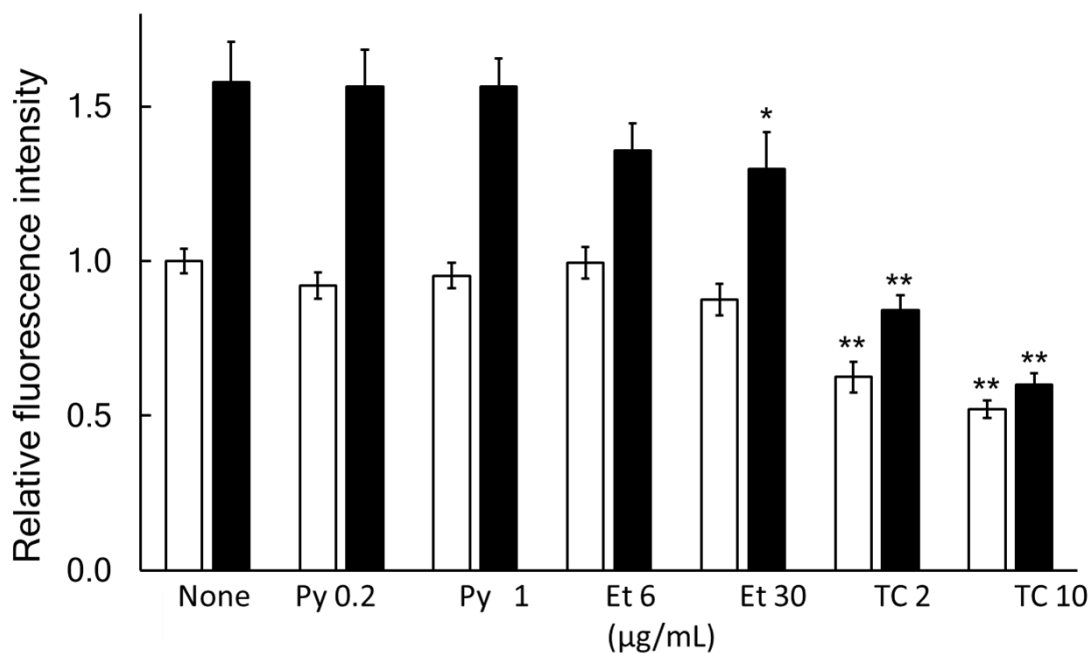
Fig. 4 Inhibition of LDs induction by inhibitors of lipid metabolism. Effect of inhibitors against lipid metabolism on LD formation in cells treated with liposomes. COS-7 cells were pre-cultured for 4 h in the presence or absence of pyrrolidine-2 (Py), etomoxir sodium (Et), and triacsin C (TC) at indicated doses respectively. After the pre-culture, DOPC/DOPE liposomes (500 μg/ml) were added and cells were cultured for 24 h. After culture, cells were stained with NR, and analyzed by flow cytometry. Open columns indicate results in the absence of liposomes, while closed columns indicate those in the presence of liposomes.

Chapter III
SR-B1 acts as a receptor for the endocytosis of phosphatidylethanolamin-containing liposomes

3.1. Abstract

As phosphatidylethanolamine (PE)-containing liposomes are very efficiently internalized in HEK293T cells, these cells were inferred to express abundant PE receptors. I examined the expression of 52 candidate genes belonging to four receptor families through transcriptome analyses, and eventually narrowed it down to four PE receptor candidate genes, which were highly expressed in HEK293T. Among siRNAs targeting these candidates, SR-B1 siRNA showed the most profound reduction in PE liposomal uptake. Conversely, the expression of SR-B1 by transfection of an expression plasmid enhanced the cellular uptake of PE-containing liposomes. A specific anti-SR-B1-antibody blocked the uptake of PE-containing liposomes in HEK293T cells. Additionally, SR-B1-Fc chimeric protein directly bound to phospholipids including PE. Lipid droplet (LD) formation in HEK293T cells induced by PE-containing liposomes was drastically suppressed by treatment with SR-B1 siRNA. After the endocytosis of PE-containing liposomes, they were co-localized with endosomes/lysosomes and SR-B1. These results indicate that SR-B1 acts as a receptor for the endocytosis of PE-containing liposomes and the induction of LDs.

3.2. Introduction

The lipid of typical mammalian cell membranes is primarily composed of phospholipids (77-80%) and cholesterol (10-20%). As phosphatidylcholine (PC), phosphatidylethanolamine (PE), phosphatidylinositol (PI), phosphatidylserine (PS), and phosphatidic acid (PA) comprise 45-55%, 15-25%, 10-15%, 5-10%, and 1-2% of the total lipids respectively, PE is the second most abundant phospholipid [1, 2, 3]. The actual proportion of these phospholipids vary considerably, depending upon tissues, cell types,

and organelles. PE is not only a major membrane constituent but also plays important regulatory roles in the synthesis and function of proteins, membrane fusion, and autophagy [2, 3].

PC is distributed symmetrically between the two leaflets of the lipid bilayer while PE and PS are more enriched in the inner leaflet than in the outer leaflet. This asymmetry is disrupted in some pathophysiological processes such as apoptosis and necrosis, leading to translocation of PE and PS from the inner to the outer leaflet [2, 3]. Redistribution of PS in the lipid bilayers in apoptotic and necrotic cells triggers a signal for the macrophages to initiate the clearance of dead cells. A number of studies have been conducted to elucidate the mechanisms by which macrophages recognize PS exposed on the surface of dead cells. Various proteins including PS receptor (PSR), T-cell immunoglobulin- and mucin-domain-containing molecule (TIM4), brain-specific angiogenesis inhibitor 1 (BAI1), stabilin-2, receptor for advanced glycation end-products (RAGE), and annexin A5 have been proposed to act as PS receptors [4, 5, 6]. However, only a few studies have been conducted to identify receptors for PE. CD300A and CD300C, which are mainly expressed on the surface of hematopoietic cells, have been reported to bind PE and transduce signals into cells [7]. Considering PE is more abundant than PS in mammalian cell membranes and apoptotic or necrotic cells express PE on the cell surface similar to PS, presumably, there may be multiple PE receptors.

I have recently reported that phospholipid nanoparticles (PNPs) are internalized into mammalian cells, and the endocytosis of PNPs promotes the formation of intracellular lipid droplets (LDs) in both non-macrophage and macrophage cell lines [8]. My study to investigate the correlation between uptake of various liposomes and their LD-inducing functions in a non-macrophage cell line, HEK293T, revealed that liposomes containing PE were very efficiently incorporated into these cells. I thus inferred that PE receptors are highly expressed in HEK293T cells. In this study, I demonstrated that scavenger receptor class B type 1 (SR-B1/SCARB1), which is the primary receptor for high density lipoproteins (HDL), acts as a PE receptor for the inducible endocytosis of PE-containing liposomes.

3.3. Materials and Methods

3.3.1. Preparation of liposomes

Liposomes were prepared according to previously described methods [8, 20, 21]. The phospholipids, DOPC, DOPS, and DOPE were purchased from the NOF corporation, and fluorescent ATTO488 (excitation: 501 nm/emission: 523 nm)-conjugated DOPE was purchased from ATTO-TEC GmbH. Briefly, an appropriate amount (e.g., 12 mg) of DOPC or a mixture of phospholipids, i.e., DOPC/DOPS (1:1 w/w), DOPC/DOPE (1:1 w/w) or DOPC/DOPE/ATTO-DOPE (10:10:1 w/w/w), was dissolved in chloroform (4 mL), and then the solution was evaporated in an eggplant-shaped flask. The flask was vortexed after adding 4 mL of phosphate-buffered saline (PBS). The resulting suspension was sonicated, and then extruded using a 100 nm pore-size membrane. The liposomal suspensions thereby obtained were dialyzed against PBS using a Spectra/Por CE dialysis tube (cut off molecular mass of 100 kDa; Repligen Co.). The suspensions were then filtered through a 0.22-µm membrane (Millipore). Particle sizes and polydispersity indices (PDIs) of liposomes were measured using the Zetasizer Nano ZS (Malvern) based on dynamic light scattering, while zeta-potentials were determined using electrophoretic light scattering. Physicochemical properties of the liposomal preparations were as follows: DOPC liposomes (particle size $=180.5 \pm 71.5$ nm; zeta potential $= -5.7 \pm 1.9$; n $= 3$), DOPC/DOPS liposome (particle size $=134.7 \pm 39.9$ nm; zeta potential $= -58.5 \pm 7.9$; n $= 7$), DOPC/DOPE liposomes (particle size $=120.2 \pm 32.1$ nm; zeta potential $= -14.1 \pm 6.9$; n $= 22$), and DOPC/DOPE/ATTO-DOPE liposomes (particle size $=164.1$ nm; zeta potential $= -31.9$; n $= 1$). PDI of all liposomes were less than 0.3. The lipid concentrations of liposomal suspensions were determined by the sulfo-phospho-vanillin method as described previously [8].

3.3.2. Cell culture

HEK293T and CHO-K1 cell lines were obtained from RIKEN RBC, Japan. They were maintained in RPMI1640 medium (Gibco) supplemented with antibiotics (penicillin and streptomycin; Gibco) and 10% heat-inactivated fetal calf serum (FCS; Biowest) in tissue culture flasks (Corning, NY, USA) or dishes (Thermo Fisher Scientific, China) in 5% CO_2 at 37 °C.

3.3.3. Fluorescence labeling of liposomes

A fluorescence-labeling reagent, CellView Claret (CV; excitation: 655 nm/emission: 675 nm; Molecular Targeting Technologies Inc.), was admixed quickly to an appropriate amount of liposomal suspension (approximately 1mg/ml in PBS) at 3.3 µL of the reagent per 1 mg of liposomes. After the mixture was incubated at 25 °C for 30 min, the resultant fluorescence-labeled liposomes were used for experiments. Labeling of liposomes by CV was done at the time of use.

3.3.4. Flow cytometric analyses to examine uptake of liposomes

To examine intracellular uptake of liposomes, HEK293T cells (2×10^5/mL) were cultured for 24 h in the presence or absence of CV-labeled liposomes in 24-well tissue culture microplates (1 mL/well; Corning). Both culture supernatant and cells were then collected from each well, and they were centrifuged in a tube at 1,500 rpm for 5 min at 22°C. Cells were washed twice with PBS by centrifugation, and then subjected to flow cytometric analyses. To detect LDs, cells were cultured in the presence or absence of unlabeled liposomes. After being cultured for 24 h, cells were collected in a tube by centrifugation, and then stained with 200 µL of Nile red solution (0.4 µg/mL in PBS) at 4 °C for 30 min according to a previously described method [8]. Fluorescence of 1.0×10^4 cells was analyzed using FACSCant II (BD Biosciences). To examine LD induction, relative fluorescence intensity was calculated by the following formula: (a-c)/(b-c); a: geometric mean of fluorescence intensity in liposome-treated cells after Nile red staining, b: geometric mean of fluorescence intensity in untreated cells after Nile red staining and c: geometric mean of fluorescence intensity of untreated cells without staining. LD induction by liposomal treatment was expressed as a relative fluorescent intensity (fold) of treated cells to that of untreated cells [8]. To evaluate liposomal uptake, I defined fluorescence intensity of cells untreated with CV-liposomes as 1.0, and uptake of liposomes was expressed as a relative fluorescent intensity (fold) of treated cells to that of untreated cells. Data were expressed as mean ± standard errors (vertical bars) in triplicate assays. Statistical analysis of Fig. 2A was done using Dunnett's test; *: p < 0.05 and **: p <0.01.

3.3.5. Fluorescence microscopy

Cells were cultured in the medium (1×10^5/mL, 300 µL/well) using an 8-well chambered cover glass (Thermo Fisher Scientific) that was pre-coated with poly-L-lysine to allow the cells to firmly adhere to the cover glass. The medium was then changed to a fresh test medium (400 µL) containing liposomes. After culture for 24 h, adherent cells were washed twice with FluoBrightTM DMEM (Gibco) and incubated in the medium containing Hoechst 33342 (excitation: 350 nm/emission: 461 nm;Thermo Fisher Scientific) to stain nuclei and LysoTracker□ Red DND-99 (excitation: 577 nm/emission: 590 nm; Thermo Fisher Scientific) to stain endosomes/lysosomes at 37 °C for 30 min in 5% CO_2. Cells were washed three times with FluoBrightTM DMEM, they were observed in FluoBrightTM DMEM under a confocal laser scanning microscope FV-1000 (Olympus) at room temperature as described before [8].

3.3.6. Transcriptome analyses of HEK293T cells

HEK293T cells (2×10^5/ml) were cultured for 24 h and the total RNA was extracted with digestion of the contaminated DNA using NucleoSpin□ RNA (Macherey-Nagel GmbH & Co. KG). cDNA libraries were constructed from the total RNA using the TruSeq stranded mRNA LT Sample Prep Kit (Illumina). Paired-end sequencing of 101 bp was performed by Macrogen Japan with a NovaSeq6000 sequencer. Total reads and Q30 (%) in trimmed data were 58,276,066 and 96.21 respectively. Processed reads (i.e., number of cleaned reads after trimming) and mapped reads to a reference genome (%) were 58,276,066 and 98.23 respectively. In case of variants, data from the longest transcript was selected. Expression data of transcripts are shown as normalized values of FPKM (Fragments Per Kilobase of transcript per Million mapped reads).

3.3.7. Suppression of liposomal uptake by siRNA

siRNA (Silencer□ Select siRNA) against glyceraldehyde-3-phosphate dehydrogenase (GAPDH), siSR-B1 (ID: s2650), scavenger receptor class B type 2 (SR-B2/SCARB2; ID: s2652), low density lipoprotein receptor-related protein 3 (LRP3; ID: s8284), annexin A5 (ANXA5; s1393) and negative control siRNA were purchased from Thermo Fisher Scientific, USA. To test the effects of these siRNAs on liposomal uptake, I pre-cultured HEK293T cells (4×104/mL) in 500 µL/ well in a 24-well tissue culture microplate at 37°C

in 5% CO_2 for 24 h. Treatment of HEK293T cells with siRNA was done using PolyMag NeoTM (Magnetofection Technology) according to the manufacture's instructions. Mixture of siRNA (1 pmole) and 0.5 µL of this reagent in Opti-MEM□ (50 µL; Gibco) was added to each well, and magnetic treatment was done for 30 min at room temperature. After cells were cultured at 37 °C in 5% CO_2 for 24 h, culture supernatant was replaced with 1 mL of fresh medium containing CV-labeled liposomes and further cultured at 37 °C in 5% CO_2 for 24 h. Fluorescence of cells incorporating liposomes was measured using a flow cytometer.

3.3.8. Reverse-transcription quantitative polymerase chain reaction (RT-qPCR)

To determine expression of SR-B1, SR-B2, LRP3, and ANXA5 mRNA in HEK293T cells, I performed RT-qPCR analyses. After treating the HEK293T cells with siRNA for 48 h, total RNA was extracted using a NucleoSpin® RNA and quantified with a spectrophotometer DS-11 (DeNovix). Reverse transcription was done with total RNA (1.2 µg) as a template using PrimeScriptTM RT Master Mix (TakaRa). Reverse-transcribed RNA (6.4 ng) was primed with oligonucleotides specific for GAPDH (5′-GAGACCCTGGTGGACATC-3′ and 5′-TTTCTTTGGTCTGCATTC-3′), SR-B1 (5′-ACAAAAGCAACATCACCTTC-3′ and 5′-TGGGCTTATTCTCCATCATC-3′), SR-B2 (5′-GTGTTAAGGAATGGTACTGAG-3′ and 5′-GAGTTCCCTGTAGGTGTATG-3′), LRP3 (5′-GTGACATGATTACCATCAGC-3′ and 5′-GAGTGGAAGAAAATCCAGAC -3′) and ANXA5 (5′-ATTAAGGGAGATACATCTGGG-3′ and 5′-GCATGCTAGTATGAATAAGGC-3′). PCR for GAPDH, SCARB1, SCARB2, and ANXA5 was done at 95 °C for 30 seconds and ran for 45 cycles at 95 °C for 10 seconds, and 60 °C for 1 min, while that for LRP3 was done at 95 °C for 30 seconds and run for 45 cycles at 95 °C for 10 sec, 55 °C for 30 sec, and 72 °C for 45 sec, with TB Green® Premix EX TaqTM II (TaKaRa) on the MyGo Pro Real Time PCR (IT-IS Life Science). All samples were assayed in triplicates and mRNA expression data was normalized on the basis of their GAPDH content. Values were expressed as means ± standard errors (vertical bars). Statistical analysis of Fig. 2B was done using Dunnett's test; *: $p < 0.05$ and **: $p < 0.01$.

3.3.9. Western blot analysis

After cells were cultured in a 24-well tissue culture plate, they were scrapped in ice-cold PBS from the plate using micropipette tips. Cells thereby collected were washed twice with PBS by centrifugation at 4 °C, and then lysed with an ice-cold RIPA buffer containing a protease inhibitor cocktail. To shear genomic DNA, each cell lysate was ultrasonicated for 1 min using a Sonifer 450AA (Branson). Protein concentration of the lysate was measured using a PierceTM BCA protein assay kit (Thermo Fisher Scientific) with bovine serum albumin (BSA) as the standard. Each lysate was mixed with a loading buffer containing bromophenol blue, sodium dodecyl sulfate (SDS), 2-mercaptoethanol, and glycerol, and then the mixture was treated at 95° C for 5 min. Resultant samples were subjected to SDS gel electrophoresis using Mini-Protean□ TGX precast gels and Tetra Systems (Bio-Rad). Precision Plus ProteinTM KaleidoscopeTM (Bio-Rad) was used as a molecular mass marker. The gel was then transferred to a polyvinylidene difluoride membrane (PVDF) using an iBlotTM (Invitrogen) or a semi-dry transfer system (Atto). Blocking of the membrane was performed in a Bullet Blocking One (Nacalai Tesque) for 5 min or in PBS containing 5% BSA and 0.05% tween 20 for 2 h at 25 °C. To detect SR-B1, the membrane was incubated with a primary antibody (a rabbit polyclonal anti-SR-B1 antibody; Gene Tex), which can recognize the C-terminal intracellular domain of SR-B1, at a dilution of 1:1,000 with a Can Get Signal□ Solution 1 (Toyobo), at 4 °C overnight. A horse radish peroxidase (HRP)-conjugated donkey polyclonal secondary antibody against rabbit IgG (GE Healthcare) was used at a dilution of 1:5,000 with a Can Get Signal□ Solution 2 (Toyobo). Treatment with the secondary antibody was performed at 25 °C for 1 h. An HRP-conjugated mouse monoclonal anti-GAPDH antibody (Wako) diluted at 1:10,000 was used to detect GAPDH as an internal control at 25 °C for 1 h. Western blot results were visualized with an AmershamTM ECLTM Prime Western Blotting Detection Reagent (GE Health) using LuminoGraph II (Atto).

3.3.10. Transfection of a plasmid to express SR-B1-GFP fusion protein

A plasmid (pCMV3-C-GFPSpark) to express SR-B1-green fluorescence protein (GFP) was purchased from Sino Biological Inc. A control plasmid to express GFP was prepared by deleting the SR-B1 open reading frame from pCMV3-C-GFPSpark. Transfection of the plasmid DNAs into cells was done using PolyMag Neo according to the manufacture's

instruction. HEK293T cells (1×10^5/mL) were precultured in 500 µL/ well in a 24-well tissue culture microplate at 37°C in 5% CO2 for 24 h. A mixture of DNA (0.4 µg) and 0.4 µl of PolyMag Neo in Opti-MEM□ (50 µL; Gibco) was added to each well and magnetic treatment was done for 20 min at room temperature. For transient expression of SR-B1-GFP or GFP alone, cells were cultured at 37°C in 5% CO2 for 6 h and then the culture supernatant was replaced with 1 mL of fresh medium containing CV-labeled liposomes. After cells were cultured at 37°C in 5% CO_2 for 18 h, they were applied to the flow cytometry to measure liposomal uptake. To obtain stable expression of SR-B1-GFP in cells, HEK293T or CHO-K1 cells were transfected with the plasmid in the same manner as described above and then cultured in the presence of hygromycin B (300 µg/ml; Invitrogen) for about one to two months. A very small number of cells expressing SR-B1-GFP survived this procedure and they were expanded for use in experiments. Stable cell lines expressing SR-B1-GFP in HEK293T cells (i.e., SR-B1-GFP-HEK) or CHO-K1 (i.e., SR-B1-GFP-CHO) were thereby established.

3.3.11. Inhibition of liposomal uptake by anti-SR-B1 antibody

HEK293T cells (1×10^5/ml) were pre-cultured in 500 µL/well in a 24-well tissue culture plate for 24 h and the culture supernatant was replaced with fresh medium (250 µL/well) containing antibody. I used a rabbit polyclonal anti-SR-B1 antibody (Abnova), which can recognize the extracellular domain of SR-B1 [11], to block SR-B1 and a rabbit polyclonal anti-phosphatidylserine (PSR) antibody (Sigma) as a control, respectively. After cells were incubated with antibodies at 37 °C in 5% CO_2 for 1 h, 250 µL of medium with or without CV-labeled DOPC/DOPE liposomes was added to each well and then they were cultured at 37°C in 5% CO_2 for 24 h. Liposomal uptake was measured using flow cytometry. Liposomal uptake of cells cultured without liposomes (control) is defined as 100% and cells cultured with antibodies are expressed as relative values to the control. Data were expressed as mean ± standard errors (vertical bars: too small to be seen in Fig. 4B) in triplicate assays. Statistical analysis was done using Student's t test; *: p < 0.05 and **: p <0.01.

3.3.12. Binding of SR-B1-Fc to phospholipids

DOPC, DOPS, or DOPE dissolved in chloroform (1mg/ml) was spotted onto a piece of AmershamTM Protran□ nitrocellulose membrane filter (GE Healthcare). The filter was treated in PBS containing 5% skim milk (Sigma) and 0.5 mM CaCl2 at 25 ℃ for 2 h, and then incubated with 2.5 µg/ml of recombinant human SR-B1-Fc chimera protein (R&D systems) in PBS containing 5% BSA and 0.5 mM $CaCl_2$ at 4 ℃ for 20 h. The filter was washed three times with PBS containing 0.5 mM $CaCl_2$, and then incubated with a HRP-conjugated rabbit polyclonal antibody to human IgG (Abcam) at the dilution of 1:5,000 with PBS containing 5% BSA and 0.5 mM $CaCl_2$ at 25 ℃ for 2 h. Visualization was done in the same manner as described in the method of western blot.

3.3.13. Assay of LD induction

Treatment with negative control siRNA and SR-B1 siRNA was performed as described above. DOPC/DOPE liposomes were added to culture 24 h after treatment with siRNAs. LD formation in HEK293T cells was measured using flow cytometry 48 h after the addition of liposomes as described previously [8]. Data were expressed as mean ± standard errors in triplicate assays. Statistical analysis was done using Student's t test; **: $p < 0.01$.

3.4. Results

3.4.1. Efficient uptake of DOPC/DOPE liposomes in HEK293T cells

I have previously reported that liposomes containing PS induce LD formation in HEK293T cells more efficiently than other liposomes not containing PS [8]. I examined the relationship between the LD-inducing functions of 1,2-dioleoyl-sn-phosphatidylcholine (i.e., DOPC), DOPC/1,2-dioleoyl-sn-glycero-3-phospho-L-serine (DOPS), and DOPC/1,2-dioleoyl-sn-phosphatidylethanolamine (DOPE) liposomes and the efficacy of liposomal uptake in HEK293T cells. As shown in Fig. 1A, DOPC/DOPS liposomes show higher LD-inducing activity than DOPC and DOPC/DOPE liposomes. However, DOPC/DOPE liposomes show significantly better efficacy of uptake than DOPC and DOPC/DOPS liposomes (Fig. 1A). No evident correlation was observed

between liposomal LD-inducing function and liposomal uptake efficacy suggesting that liposomes of different constituents are incorporated into HEK293T cells in a different manner. During these experiments, I unexpectedly found that HEK293T cells were able to incorporate PE-containing liposomes very efficiently. I examined intracellular distribution of DOPC/DOPE liposomes in HEK293T cells under a fluorescence microscope. As shown in Fig. 1B, the majority of CV-derived fluorescence of the liposomes and endosomes/lysosomes were co-distributed in the cytoplasm.

3.4.2. Transcriptome analysis of HEK293T cells and suppression of DOPC/DOPE uptake by siRNA targeting SR-B1

Based on the above results, I inferred that HEK293T cells abundantly express PE receptors responsible for the endocytosis of PE-containing liposomes. I performed transcriptome analyses of HEK293T cells to identify candidate genes encoding PE receptors. I focused on the transcripts from four receptor families: reported PE receptors, scavenger receptors, low density lipoprotein receptor (LDLR) family, and reported PS receptors, because some of these gene products have been reported to bind phospholipids [9]. The expression profile of 52 transcripts from these receptor families is shown in Fig. 2A. I selected four candidate genes which were highly expressed in HEK293T cells (SR-B1, SR-B2, LPR3, and ANXA5; asterisks in Fig. 2A) and prepared siRNAs targeting these genes. Fig. 2B shows that these siRNAs specifically suppressed SR-B1, SR-B2, LRP3, and ANXA5 mRNA expression.

I examined the effects of the negative control, GAPDH, SR-B1, SR-B2, LRP3, and ANXA5 siRNAs, on liposomal uptake by HEK293T cells (Fig. 2C). The highest reduction in liposomal uptake was observed for DOPC/DOPE liposomes which was reduced to 24.1% by SR-B1 siRNA. These results suggest that SR-B1 mainly acts as a receptor for PE. In addition, SR-B1 siRNA marginally suppressed DOPC/DOPS and DOPC liposomal uptakes. These results were consistent with a previous report showing that SR-B1 can act as a receptor for PS [10].

Subsequently, I examined effect of SR-B1 siRNA on protein expression by western blot. As shown in Fig. 2D, SR-B1 was detected at approximately 75 kDa. Treatment with SR-B1 siRNA evidently reduced the expression of both SR-B1 protein and SR-B1 mRNA.

3.4.3. Enhancement of DOPC/DOPE liposomal uptake in cells by expression of SR-B1

I transfected a plasmid to express SR-B1-GFP fusion protein into HEK293T cells and examined the effect of its expression on liposomal uptake. A liposomal uptake experiment was performed within 24 h after the introduction of plasmid DNA for the transient expression of SR-B1-GFP in HEK293T cells, since expression of SR-B1-GFP did not influence cell growth and viability during this time period. As shown in Fig. 3A (2nd and 4th rows), expression of SR-B1-GFP apparently enhances DOPC, DOPC/DOPS and DOPC/DOPE liposomal uptake by 3.1-, 4.3-, and 7.2-folds respectively in GFP-positive cells (GFP+) compared to GFP-negative cells (GFP-) as inferred from their geometric mean values of fluorescence intensities. However, expression of GFP without SR-B1 did not increase liposomal uptakes (Fig. 3A, 3rd and 5th rows) indicating that SR-B1 alone is responsible for the enhancement of liposomal uptake.

The enhancement of DOPC/DOPE liposomal uptake was observed in CHO-K1 cells too, stably expressing SR-B1-GFP. Similar enhancement in DOPC/DOPS and DOPC/DOPE liposomal uptake was detected in CHO-K1 cells (i.e., 2.2- and 4.6-fold increase, respectively) caused by the expression of SR-B1-GFP (Fig. 3B). However, enhancement in DOPC liposomal uptake was not observed.

I compared the expression levels of SR-B1-GFP protein in HEK293T and CHO-K1 cells by western blot. SR-B1-GFP protein bands were detected at the position of expected molecular mass (approximately 102 kDa) in both HEK293T and CHO-K1 cells transfected with the plasmid (Fig. 3C). Expression levels of SR-B1-GFP protein were greater in HEK293T cells than in CHO-K1 cells which would explain the smaller increase in liposomal uptake in CHO-K1 cells compared to that in HEK293T cells.

3.4.4. Endocytosis and LD formation induced by DOPC/DOPE liposomes in HEK293T cells via SR-B1

SR-B1 functions as the primary receptor for high density lipoprotein (HDL) and has the ability to transport cholesterol esters from HDL by a non-endocytic process referred to as selective uptake [11]. Although I showed that CV-derived fluorescence of DOPC/DOPE liposomes was co-localized with endosomes/lysosomes (Fig. 1 B), the possibility that CV was solely transported to the cytoplasm without endocytosis of the liposomes could not be ruled out. I therefore prepared DOPC/DOPE/ATTO-DOPE

liposomes in which phospholipids covalently conjugated to a fluorescent moiety ATTO-DOPE were integrated into the lipid bilayers of liposomes. Co-distribution of liposomes and endosomes/lysosomes was observed upon culturing HEK293T cells in the presence of these liposomes (Fig. 4A) which indicated that PE-containing liposomes were certainly endocytosed by HEK293T cells.

To confirm that the interaction of DOPC/DOPE liposomes to SR-B1 was indispensable for the uptake of DOPC/DOPE liposomes in HEK293T cells, I examined the effect of an anti-SR-B1 antibody, which has been reported to block the binding of HDL or LDL to SR-B1 [12] upon uptake of DOPC/DOPE liposomes by HEK293T cells. This antibody inhibits DOPC/DOPE liposomal uptake by HEK293T cells in a dose-dependent manner whereas a control antibody, a polyclonal anti-PSR antibody [13], failed to inhibit this uptake (Fig. 4B). I tested direct binding of SR-B1 to DOPE using SR-B1-Fc chimeric protein. As shown in Fig. 4C, SR-B1-Fc bound to various phospholipids including DOPE, although its binding to DOPC was stronger than those to DOPE and DOPS. These results indicate that DOPC/DOPE liposomes can directly bind to SR-B1 as a ligand and induce the endocytosis of these liposomes.

I have previously reported that DOPC/DOPE liposomes induce LD formation in HEK293T cells. I examined whether not only endocytosis but also LD formation induced by DOPC/DOPE liposomes are controlled via SR-B1. As shown in Fig. 4C, SR-B1 siRNA drastically reduced LD formation induced by DOPC/DOPE liposomes. These results indicated that interaction between DOPC/DOPE liposomes and SR-B1 causes LD formation induced by PE-containing liposomes.

3.4.5. Co-distribution of DOPC/DOPE liposomes, endosomes/lysosomes, and SR-B1 in HEK293T cells

I examined the cellular distributions of SR-B1-GFP and CV-labeled DOPC/DOPE liposomes after culturing SR-B1-GFP-HEK cells in the presence of CV-labeled DOPC/DOPE liposomes. As shown in Fig. 5A, co-distribution of liposomes and endosomes/lysosomes was observed which were consistent to Fig. 1B and Fig. 4A. Not only endosomes/lysosomes and SR-B1-GFP but also CV-DOPC/DOPE and SR-B1-GFP were co-localized in the cytoplasm as shown in Fig. 5B and Fig. 5C respectively. In addition, co-localization of CV-DOPC/DOPE and SR-B1-GFP was detected in the

vicinity of the cell membrane (Fig. 5C). In contrast, co-localization was not observed between CV-DOPC/DOPE and GFP (Fig. 5D). Taken together, my results indicate that DOPC/DOPE liposomes were endocytosed into endosomes/lysosomes together with SR-B1.

3.5. Discussion

In this study, I demonstrated for the first time that SR-B1 acts as a PE receptor to efficiently cause the endocytosis of liposomes containing PE. CD300A/C have been reported to function as receptors for PE [7]. However, CD300A/C genes were not abundantly expressed in HEK293T cells (i.e., FMKM of 0 and 0.026, respectively in Fig. 2A). Expression of these genes is restricted to hematopoietic lineage cells. In contrast, SR-B1 is expressed in a wide variety of cells including adipocytes, monocytes/macrophages, endothelial cells, keratinocytes, epithelial cells, and smooth muscle cells [14], suggesting that SR-B1 might function as a PE receptor in a wider variety of cells and tissues than CD300A/C. Although SR-B1 functions as a PE receptor inducible endocytosis of PE-containing liposomes, my data does not rule out the possibility that SR-B1 can act as PC or PS receptors too. However, the efficacy of SR-B1 as a PC or PS receptor would be lower than that as a PE receptor. SR-B1 has been reported to interact with various ligands including PS and oxidized phospholipids [10, 11, 14]. In a previous report, binding of [^{3}H]-labeled PS-containing liposomes to SR-B1 was inhibited by PS-containing liposomes whereas PE-containing liposomes failed to inhibit [^{3}H]-labeled PS liposomal binding to SR-B1 [10]. Binding sites of PS and PE to SR-B1 might differ. In addition, I showed that SF-B1-Fc bound to not only DOPE but also DOPS and DOPC. The results of this study are consistent to the previous reports demonstrating SR-B1 acts as receptors for various phospholipids [10, 11, 14]. The binding of SR-B1-Fc to DOPC was stronger than DOPE and DOPC, suggesting that the binding activity of phospholipids to SR-B1 does not necessarily reflect the efficacy of liposomal uptake. In addition, the results of siRNA experiments demonstrated that LD formation induced by PE-containing liposomes is via SR-B1, which indicate that PE can modulate cellular functions through SR-B1.

PE as well as PS are redistributed in the cell membrane during apoptotic and necrotic cell death and the both phospholipids become exposed on the cell surfaces of dead cells. Similar to PS, PE would play an important role as a signal to induce clearance of dead and malfunctional cells. Indeed, CD300A has been suggested to bind dead cells via PE and to contribute to dead cell clearance by macrophages [15, 16]. In addition, SR-B1 has been reported to mediate endocytosis of apoptotic cells by CHO-AL1 cells [11, 17]. PE and SR-B1 interaction might also be related to apoptotic cell clearance, although it should be confirmed by future studies.

PE is a representative component used for liposomal carriers in DDS. In particular, cationic liposomes are frequently used as a carrier to deliver nucleic acids into cells. DOPE has been added to these liposomes to enhance transfection efficacy, although DOPE is a neutral phospholipid [18]. DOPE increases permeability and fusogenicity in lipid bilayers [19] so the enhancement in transfection efficacy by DOPE has been attributed to its physicochemical properties. Re-evaluation of DOPE with respect to its interaction with SR-B1 would be necessary.

3.6. References

1. Vance, J.E. 2015. Phospholipid synthesis and transport in mammalian cells. Traffic.16:1-18. doi: 10.1111/tra.12230.

2. Calzada, E., O. Onguka, and S.M. Claypool. 2016. Phosphatidylethanolamine Metabolism in Health and Disease. Int. Rev. Cell Mol. Biol. 321:29-88. doi: 10.1016/bs.ircmb.2015.10.001.

3. van der Veen J.N., J.P. Kennelly, S. Wan, J.E. Vance, D.E. Vance, and R.L. Jacobs. 2017. The critical role of phosphatidylcholine and phosphatidylethanolamine metabolism in health and disease. Biochim. Biophys. Acta. Biomembr. 1859:1558-1572. doi: 10.1016/j.bbamem.2017.04.006.

4. Zhou, Z. 2007. New phosphatidylserine receptors: clearance of apoptotic cells and more. Dev. Cell. 13:759-760.

5. Armstrong, A., and K.S. Ravichandran. 2011. Phosphatidylserine receptors: what is the new RAGE? EMBO Rep. 12:287-288. doi: 10.1038/embor.2011.41.

6. Crowley, L.C., B.J. Marfell, A.P. Scott, and N.J. Waterhouse. 2016. Quantitation of Apoptosis and Necrosis by Annexin V Binding, Propidium Iodide Uptake, and Flow Cytometry. Cold Spring Harb Protoc. doi: 10.1101/pdb.prot087288.

7. Takahashi, M., K. Izawa, J. Kashiwakura, Y. Yamanishi, Y. Enomoto, A. Kaitani, A. Maehara, M. Isobe, S. Ito, T. Matsukawa, F. Nakahara, T. Oki, M. Kajikawa, C. Ra, Y. Okayama, T. Kitamura, and J. Kitaura. 2013. Human CD300C delivers an Fc receptor-γ-dependent activating signal in mast cells and monocytes and differs from CD300A in ligand recognition. J. Biol. Chem. 288:7662-7675. doi: 10.1074/jbc.M112.434746..

8. Fujita, K., M. Somiya, S. Kuroda, and S. Hinuma. 2019. Induction of lipid droplets in non-macrophage cells as well as macrophages by liposomes and exosomes. Biochem. Biophys. Res. Commun. 510:184-190. doi: 10.1016/j.bbrc.2019.01.078.

9. Penberthy, K.K., and K.S. Ravichandran. 2016. Apoptotic cell recognition receptors and scavenger receptors. Immunol. Rev. 269:44-59. doi: 10.1111/imr.12376.

10. Rigotti, A., S.L. Acton, and M. Krieger.1995. The class B scavenger receptors SR-BI and CD36 are receptors for anionic phospholipids. J. Biol. Chem. 270:16221-16224.

11. Shen, W.J., S. Asthana, F.B. Kraemer, and S. Azhar. 2018. Scavenger receptor B type 1: expression, molecular regulation, and cholesterol transport function. J. Lipid Res. 59:1114-1131. doi: 10.1194/jlr.R083121.

12. Gu, X., K. Kozarsky, and M. Krieger. 2000. Scavenger receptor class B, type I-mediated [^{3}H]cholesterol efflux to high and low density lipoproteins is dependent on lipoprotein binding to the receptor. J. Biol. Chem. 275:29993-30001.

13. Zakharova, L., M. Svetlova, and A.F. Fomina. 2007. T cell exosomes induce cholesterol accumulation in human monocytes via phosphatidylserine receptor. J. Cell Physiol. 212:174-181.

14. Ashraf, M.Z., N.S. Kar, X. Chen, J. Choi, R.G. Salomon, M. Febbraio, and E.A. Podrez. 2008. Specific oxidized phospholipids inhibit scavenger receptor bi-mediated selective uptake of cholesteryl esters. J. Biol. Chem. 283:10408-10414. doi: 10.1074/jbc.M710474200.

15. Simhadri VR, Andersen JF, Calvo E, Choi SC, Coligan JE, Borrego F. 2012 Human CD300a binds to phosphatidylethanolamine and phosphatidylserine, and modulates

the phagocytosis of dead cells. Blood. Mar 22;119(12):2799-809. doi: 10.1182/blood-2011-08-372425.

16. Zenarruzabeitia, O., Vitallé, J., Eguizabal, C., Simhadri, V.R., and Borrego F. 2015. The biology and disease relevance of CD300a, an inhibitory receptor for phosphatidylserine and phosphatidylethanolamine. J. Immunol. 1;194(11):5053-60. doi: 10.4049/jimmunol.

17. Fukasawa, M., Adachi, H., Hirota, K., Tsujimoto, M., Arai, H., and K. Inoue. 1996. SRB1, a class B scavenger receptor, recognizes both negatively charged liposomes and apoptotic cells. Exp. Cell Res. 222:246-250.

18. Mochizuki, S., N. Kanegae, K. Nishina, Y. Kamikawa, K. Koiwai, H. Masunaga, and K. Sakurai. 2013. The role of the helper lipid dioleoylphosphatidylethanolamine (DOPE) for DNA transfection cooperating with a cationic lipid bearing ethylenediamine. Biochim. Biophys. Acta. 1828:412-418. doi: 10.1016/j.bbamem.2012.10.017.

19. Chen, Z., and R.P. Rand. 1997. The influence of cholesterol on phospholipid membrane curvature and bending elasticity. Biophys. J. 73:267–276

20. Amano, C., H. Minematsu, K. Fujita, S. Iwashita, M. Adachi, K. Igarashi, and S. Hinuma. 2015. Nanoparticles Containing Curcumin Useful for Suppressing Macrophages In Vivo in Mice. PLoS One. doi: 10.1371/journal.pone.0137207.

21. Fujita, K., Y. Hiramatsu, H. Minematsu, M. Somiya, S. Kuroda, M. Seno, and S. Hinuma. 2016. Release of siRNA from Liposomes Induced by Curcumin. J. Nanotechnology doi: 10.1155/2016/7051523

3.7. Figures and legends
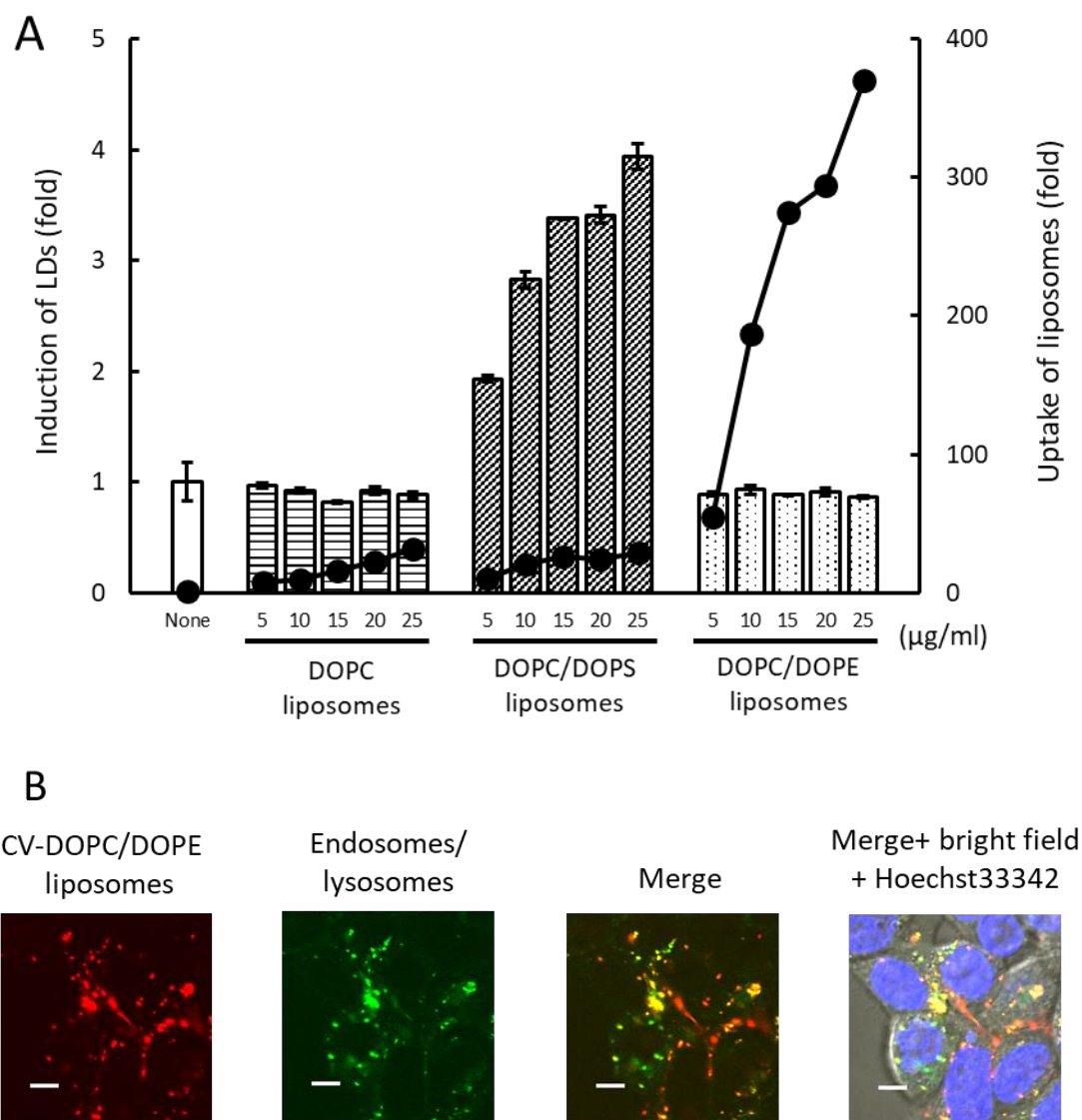
Fig. 1 Efficient uptake of DOPC/DOPE liposomes by HEK293T cells. A: Cells were cultured with or without indicated doses of CV-labeled liposomes, and liposomal uptake (●) was analyzed using flow cytometry. Columns indicate the levels of LDs. B: Cells were treated with CV-labeled DOPC/DOPE liposomes (25 µg/mL). After endosomes/lysosomes and nuclei were stained, they were subjected to fluorescence microscopic analyses to examine localization of CV-DOPC/DOPE liposomes (red) and endosomes/lysosomes (green). Merge: merged images of CV-liposomal and endosomal/lysosomal distributions. Merge + bright filed + Hoechst 33342: merged images of Merge, bright field, and nuclei (blue). Bars indicate 5 µm.

A

B

GAPDH mRNA   SR-B1 mRNA   SR-B2 mRNA   LRP3 mRNA   ANXA5 mRNA

siRNA treatment
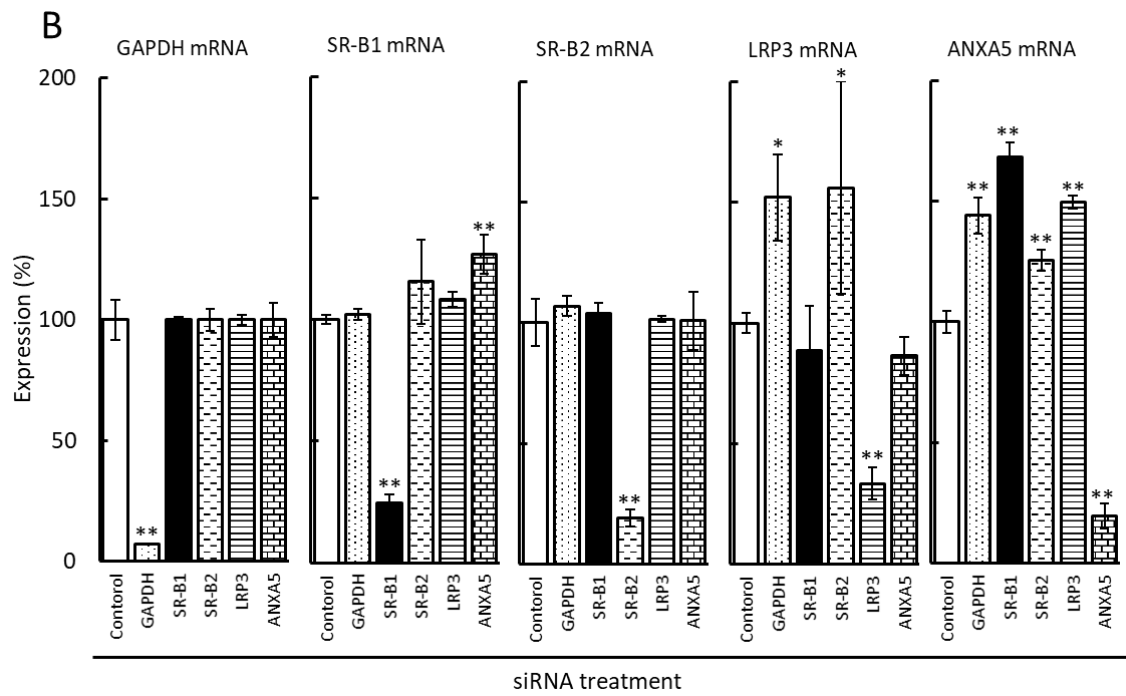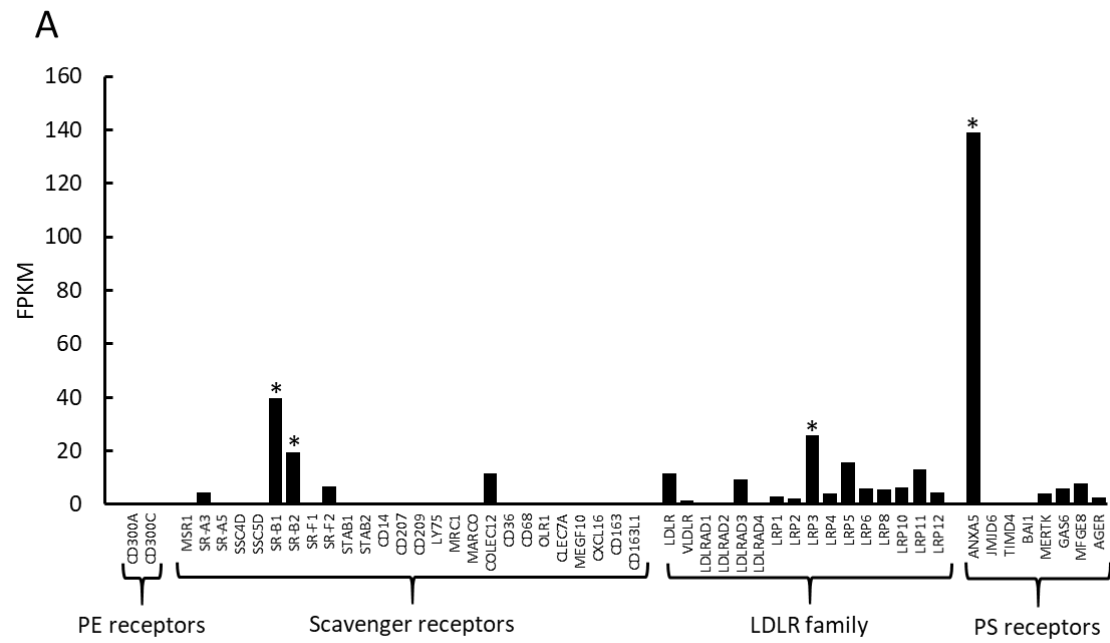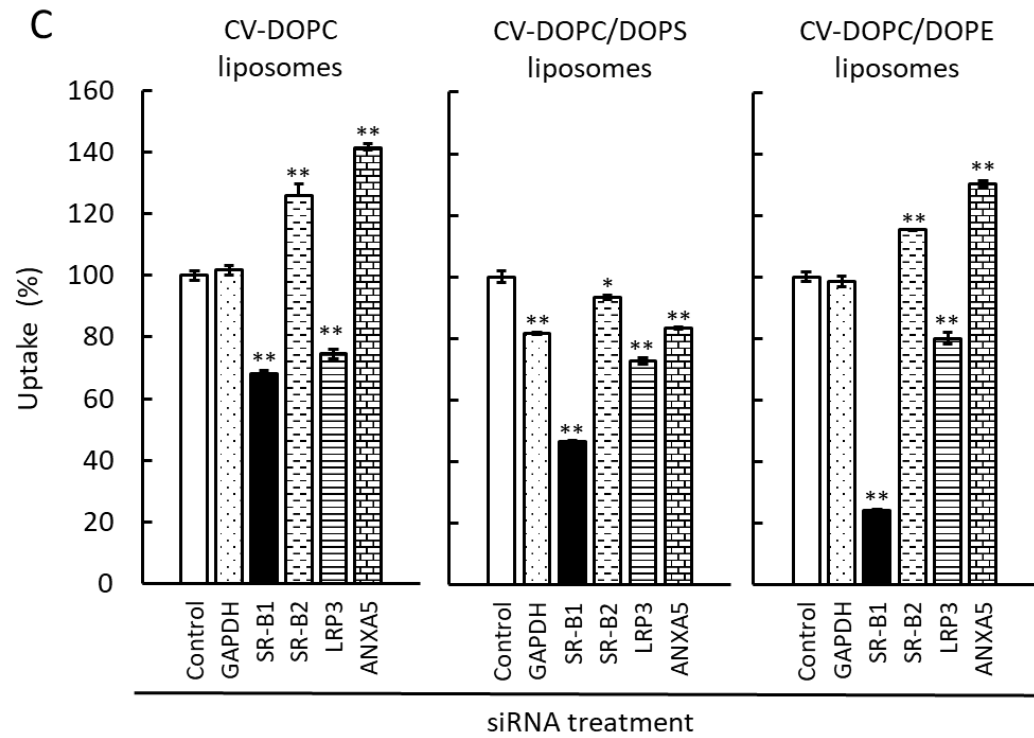
Fig. 2 Gene expression profile of HEK293T cells and preparation of siRNAs targeting candidate genes encoding PE receptors (A, B). A: The indicated four receptor families were extracted from transcriptome data and their gene expression levels are shown as FPKM. Four genes indicated with asterisks were subsequently subjected to siRNA experiments. B: Ater 24 h treatment of cells by indicated siRNAs, expression levels of indicated mRNAs were determined using RT-qPCR. Expression of mRNA after treatment with the negative control siRNA is defined as 100%, and those after treatment with indicated siRNAs are shown as relative values to the control. C: After treatment of cells

by indicated siRNAs, these cells were cultured with CV-labeled liposomes. Liposomal uptakes were measured using flow cytometry. Liposomal uptake after treatment with the negative control siRNA is defined as 100%, and those after treatment with indicated siRNAs are shown as relative values to the control. D: Cells were cultured for 48 h after treatment with or without control or SR-B1 siRNA, and then proteins (2.4 µg/lane) extracted from the cells were subjected to western blot analyses. The position of SR-B1 (the upper picture) and GAPDH (the lower picture) are shown by arrowheads. Molecular mass markers are shown at the left of the picture.

A
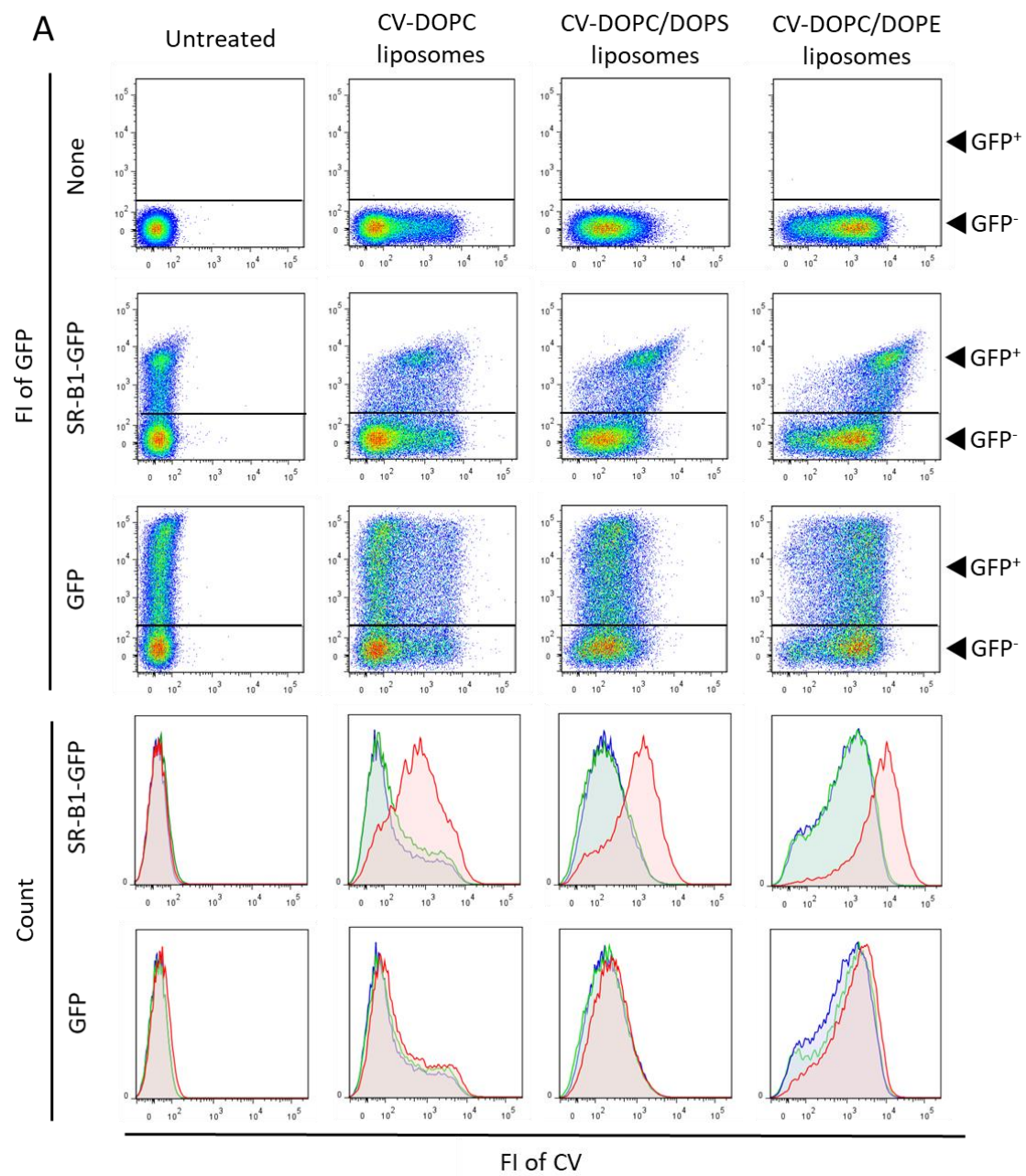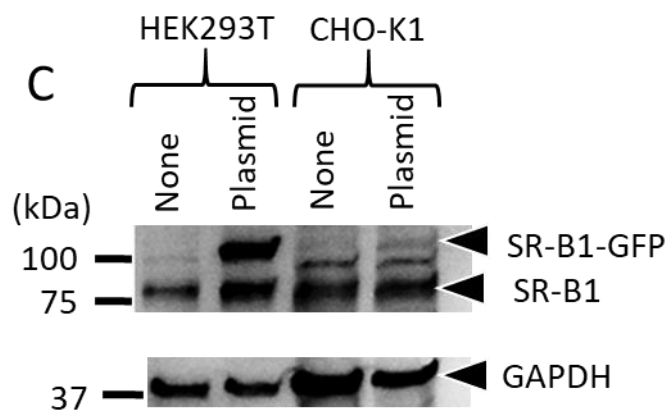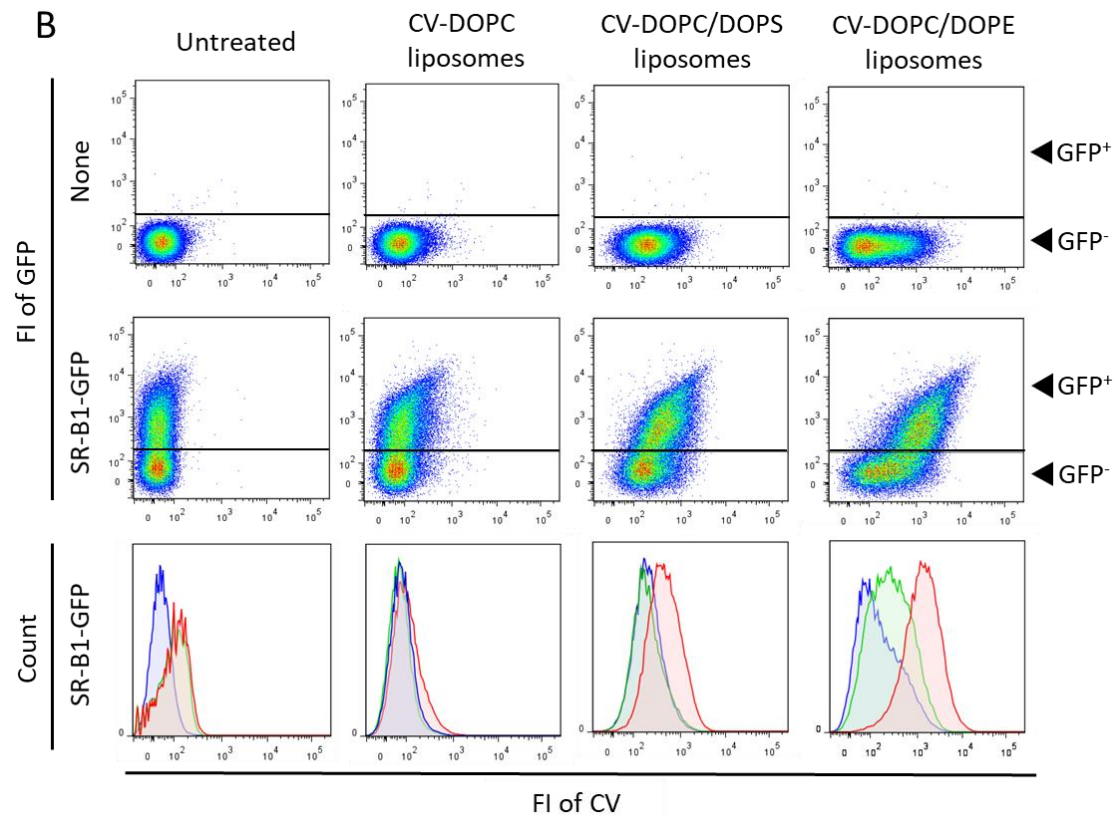
Fig. 3 Enhancement of liposomal uptake in cells by expression of SR-B1-GFP fusion protein. A: SR-B1-GFP or GFP alone was transiently expressed in HEK293T cells by transfection of plasmids. Six hours after transfection with expression plasmids, indicated CV-labeled liposomes (3.8 μg/mL) were added to the cells. These were cultured in the absence (None) or presence of CV-labeled liposomes for 18 h and then fluorescence intensities (FI) of GFP and CV in 50,000 cells were analyzed using flow cytometry. The 1st, 2nd and 3rd row panels indicate unexpressed, SR-B1-GFP- and GFP-expressed cells,

56

respectively. FI of cells are shown as densities of dots (i.e., blue < green < red) in two-parameter plots (in log scale). GFP-positive (GFP+) and GFP-negative (GFP-) populations indicated by arrowheads are gated. Histograms of SR-B1-GFP- and GFP-expressed cells are shown in the 4th and 5th row panels. In these histograms, GFP-populations in unexpressed cells and those in SR-B1-GFP- in SR-B1-GFP-expressed cells are indicated as blue and green areas respectively, while GFP+ populations in SR-B1-GFP-expressed cells are indicated as red areas. B: SR-B1-GFP was stably expressed in CHO-K1 cells. They were cultured in the absence (None) or presence of CV-liposomes for 24 h. Flow cytometric analyses were then performed. D: After transfection of an expression plasmid of SR-B1-GFP, its expression was examined by western blot analysis. HEK293T cells were cultured for 24 h after treatment with (Plasmid) or without (None) the SR-B1-GFP-expression plasmid. On the other hand, CHO-K1 cells transfected with (Plasmid) or without (None) were cultured for 24 h. Protein samples prepared from HEK293T cells and CHO-K1 cells were subjected to SDS gel electrophoresis at 2.4 and 9.6 µg/lane respectively. Stained bands on the membrane at the position of SR-B1-GFP, SR-B1 (the upper picture) and GAPDH (the lower picture) are shown by arrowheads. Molecular mass markers are shown at the left of the picture.
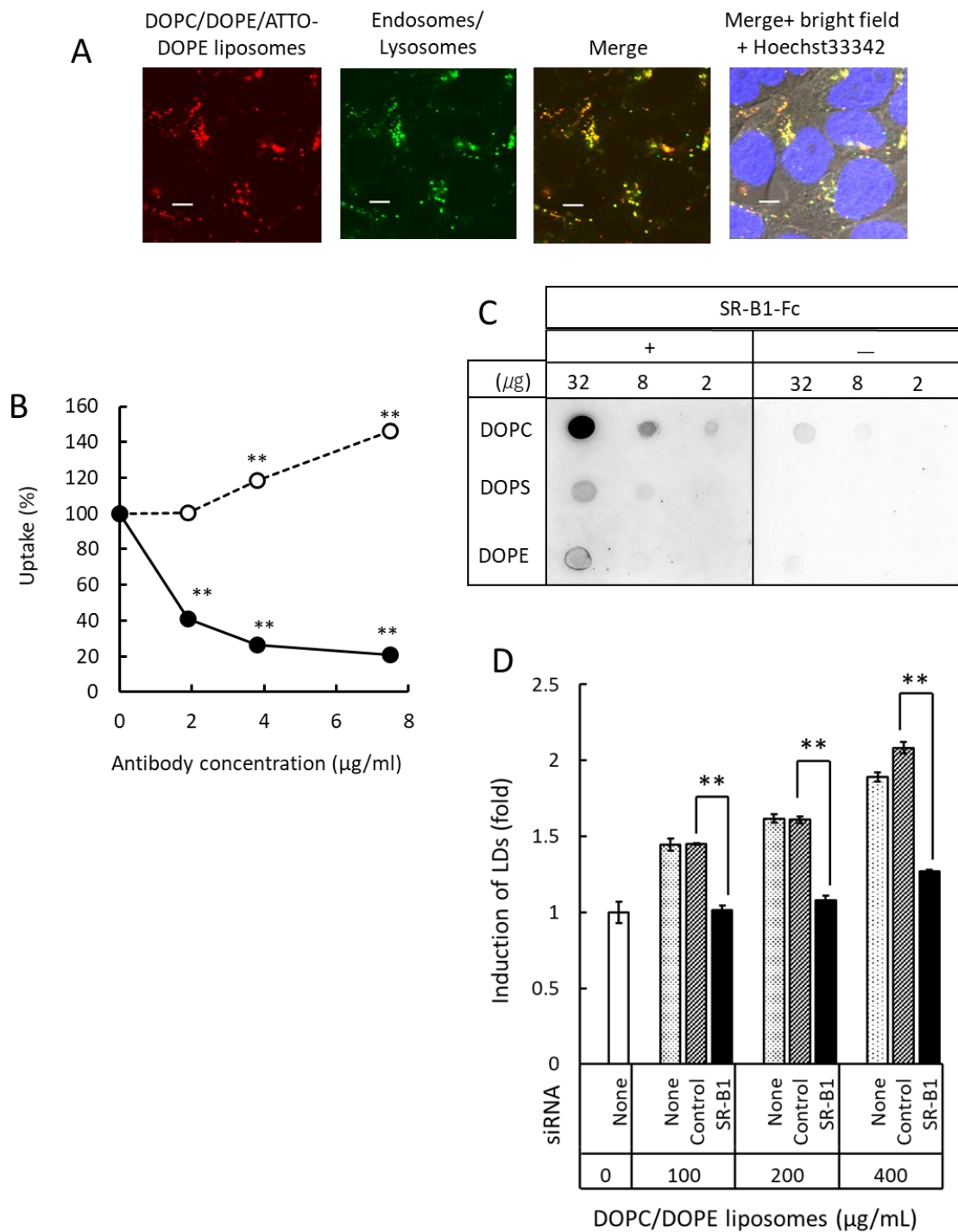
Fig. 4 Endocytosis of DOPC/DOPE liposomes via SR-B1. A: HEK293T cells were cultured in the presence of DOPC/DOPE/ATTO-DOPE liposomes (25 µg/ml) for 24 h. Localization of DOPC/DOPE/ATTO-DOPE liposomes (red) and endosomes/lysosomes (green) in the cells was examined. Merge: merged images of DOPC/DOPE/ATTO-DOPE liposomal and endosomal/lysosomal distributions; merge + bright filed + Hoechst 33342:

58

merged images of Merge, bright field, and nuclei (blue). Bars indicate 5 μm. B: Inhibition of DOPC/DOPE liposomal uptake in HEK293T cells by anti-SR-B1 antibody. HEK293T cells were treated with anti-SR-B1 (●) or anti-PSR antibodies (○). These were cultured in the presence of CV-DOPC/DOPE liposomes (3.8 µg/mL) and then liposomal uptake was analyzed using flow cytometry. C: Binding of SR-B1-Fc chimeric protein to DOPC, DOPS, and DOPE are shown. Indicated amounts of each phospholipid was spotted onto nitrocellulose filter strips. After incubation of the filter with (+) or without (-) SR-B1-Fc, its binding to phospholipids was detected using an HRP-anti-IgG antibody. D: Suppression of DOPC/DOPE liposome-induced LD formation by SR-B1 siRNA. Cells cultured in a 24-well plate were treated with or without negative control or SR-B1 siRNA for 24 h, and then the indicated amounts of DOPC/DOPE liposomes were added to the culture. Forty-eight hours after the addition of the liposomes, cells were stained using Nile red. LD induction was measured using flow cytometer. Blank, dotted, shaded, and filled columns indicate untreated, addition of liposomes, addition of liposomes after negative control siRNA treatment, and addition of DOPC/DOPE liposomes after SR-B1 siRNA treatment respectively. Fluorescent intensity of untreated cells was defined as 1.0. LD induction in cells by liposomes is indicated as a ratio to the untreated cells.
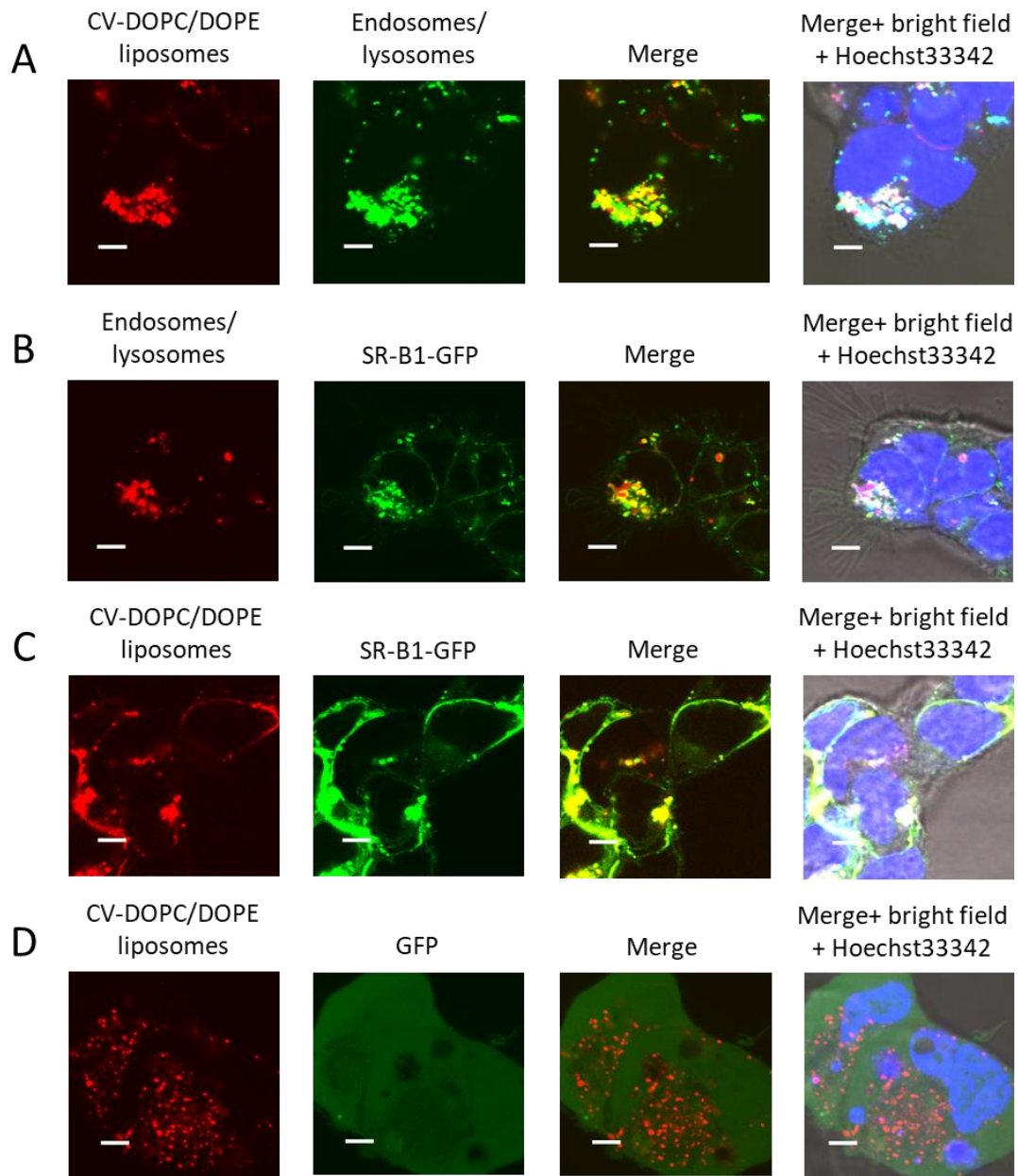
Fig. 5 Distribution of DOPC/DOPE liposomes, endosomes/lysosomes, and SR-B1 in HEK293T cells. SR-B1-GFP-HEK (D – F) or GFP-HEK (G) cells were cultured in the presence of CV-DOPC/DOPE liposomes (7.5 µg/mL) for 24 h. A: Distributions of CV-DOPC/DOPE liposomes (red) and endosomes/lysosomes (green); merge: merged images of CV-DOPC/DOPE liposomal and endosomal/lysosomal distributions; merge + bright filed + Hoechst 33342: merged images of Merge, bright field, and nuclei (blue) (A – D). Bars indicate 5 µm (A – D). B: Distributions of endosomes/lysosomes (red) and SR-B1-GFP (green); merge: merged images of endosomal/lysosomal and SR-B1-GFP distributions. C: Distributions of CV-DOPC/DOPE liposomes (red) and

60

endosomes/lysosomes (green); merge: merged images of CV-DOPC/DOPE liposomal and endosomal/lysosomal distributions. D: Distributions of CV-DOPC/DOPE liposomes (red) and GFP (green); merge: merged images of CV-DOPC/DOPE liposomal and GFP distributions.

Chapter IV
Effect of liposomes on cell survival under glucose-deficient conditions

4.1 Abstract

In this study, I examined the effects of liposomes on lipid droplet (LD) formation and the promotion of cell survival in L929 cells under glucose-deficient conditions. LD formation was analyzed using flow cytometry and microscopy while cell survival was determined using the trypan blue dye exclusion test and flow cytometry. In cell culture, glucose facilitated liposome-induced LD formation in a dose-dependent manner. In a culture of complete glucose deprivation, liposomes did not induce LD formation or evident survival in cells. However, in the presence of low-dose glucose in culture, liposomes promoted cell survival, indicating that liposomes and low-dose glucose synergistically promote cell survival. Liposomes containing phosphatidylserine showed greater activities of cell survival promotion and LD induction than those containing phosphatidylethanolamine. These results suggest that cell survival promotion and LD formation induced by liposomes are closely related.

4.2 Introduction

Lipid droplets (LDs) are organelles found ubiquitously in mammalian cells. LDs are produced from the lipid bilayers of the endoplasmic reticulum membranes through a budding-like process [1]. LDs contain triacylglycerol (TAG) and sterol esters in the core. Therefore, LDs had been considered simply as organelles to store lipids. However, recent studies indicate that LDs have a variety of regulatory roles in not only energy metabolism but also various other functions including mitigation against stress. It has been reported that LDs are induced in cells in response to nutrient deprivation and that cell death is accelerated by inhibiting the biosynthesis of LDs [2]. Through the processes of lipolysis or autophagy, LDs are considered a supplier of fatty acids that are necessary for energy synthesis and the fatty acids are metabolized through β oxidation and the citrate cycle in mitochondria and peroxisomes. In this way, LDs are thought to promote cell survival under conditions of nutrient deprivation [3- 7].

Glucose is the most representative carbohydrate as a source of energy in mammalian cells. After glucose is taken up into cells via glucose transporters such as GlUT4 on the cell membrane, it is catabolized through the first step of the pathway referred to as glycolysis which begins with the generation of glucose-6-phosphate and ends the production of pyruvate. Through glycolysis, two ATPs are produced by the phosphorylation of two ADPs. Under aerobic conditions, pyruvates produced by glycolysis enter into the second step of the tricarboxylic acid (TCA) cycle pathway, in the mitochondria. Electrons derived from metabolites of the TCA cycle transferred to the electron transport chain (ETC) which are protein complexes embedded in the mitochondrial inner membrane. During transfer of electrons in ETC, protons are accumulated in the space between inner and outer mitochondrial membrane. ATP synthetase integrated in the inner membrane produces ATP from ADP using the flow of protons across the inner membrane. Efficacy of ATP production is far greater in mitochondria than in glycolysis. In total, 36 ATP are produced through the all catabolic processes of glucose [12].

Fatty acids are another important energy source of cells. A single C18 fatty acid can produce 90 ATP through synthesis of acetyl-CoA in β oxidation [13]. In glucose deprivation, metabolites derived from fatty acid oxidation are served for aerobic energy metabolism [14]. As described in Chapter II, I demonstrated that phospholipid nanoparticles (PNPs) including liposomes and exosomes can induce LDs in non-macrophage cells as well as macrophages [8]. Because LDs are a potential source of fatty acids, it is interesting whether LDs induced by PNPs influence cellular responses against glucose deprivation. In this study, I examined the effects of liposomes on the survival of a mouse fibroblast cell line (L929) under glucose-deficient conditions.

4.3 Material and Methods

4.3.1. Preparation of liposomes
Liposomes were prepared according to the methods described in Chapter II.

4.3.2. Cell culture

L929 (a mouse fibroblastic cell line) was obtained from Japan Health Science Foundation. These cells were maintained in RPMI1640 medium containing L-glutamine and HEPES (Gibco) supplemented with antibiotics (penicillin and streptomycin; Gibco) and heat-inactivated10% fetal calf serum (FCS; Biowest) in tissue culture flasks (Corning) or dishes (Nunc) in 5% CO_2 at 37 °C. To culture under glucose-deficient conditions, cells were washed twice with phosphate-buffered saline (PBS) by centrifugation, and then these were suspended in a medium that is glucose-free RPMI1640 medium containing L-glutamine and HEPES (Gibco) supplemented with antibiotics (penicillin and streptomycin; Gibco) and 10% dialyzed FCS (Biowest). To examine the effects of liposomes on cultured cells, I diluted liposomal suspensions with PBS and then admixed them with an equal volume of cell suspension. The mixture of cell suspension in the medium and liposomal suspension in PBS is referred to as 'test medium' in this study. If necessary, I adjusted the glucose concentration of the cell culture in the test medium by the addition of a glucose solution in PBS (10 mg/ml).

4.3.3. Trypan blue dye exclusion test

After L929 cells were cultured in the test medium (100 µl /well) with or without liposomes in a 96-well plate, trypan blue solution was added, and then cell images were captured with a CCD camera (Visualix-Pro2; Visualix) under an inverted microscope (CKX41; Olympus). Cell viability was analyzed from the images with software (Nihon system developer Co).

4.3.4. Flow cytometric analyses

Cells were cultured in the test medium (2 ml/well) with or without liposomes in a 12-well tissue culture microplate (Corning). All cells were washed once with PBS and then harvested from the plate by trypsinization. The cell suspension was centrifuged in a tube at 1,500 rpm for 5 min at 4 °C using the KUBOTA2700 (Kubota) and washed once with PBS. To detect LDs in cells, live cells were stained with 200 µl of NR solution (0.4 µg/ml in PBS) at 4 °C for 40 min according to a previously described method [11]. In each specimen, the fluorescence of 1.0×10^4 cells was analyzed. The intensity of intracellular fluorescence in each specimen was measured as a geometric mean. To access apoptotic

cells, I used a FAM-FLICA (fluorescent-labeled inhibitor of caspases) poly caspase kit (Bio-Rad) according to the manufacturer's instructions. After staining with FAM-FLICA and propidium iodine, all specimens were washed twice with a washing buffer by centrifugation, fixed with adding a fixation buffer, and subjected to flow cytometric analyses using FACScant II (BD Biosciences). Before subjecting these follow cytometric assays, I recorded cell images in culture using an inverted microscope CKX41 (Olympus) equipped with a CCD camera Visualix-Pro2A (Visualix).

4.4 Result

4.4.1. LD induction in cells by liposomes under glucose-deficient conditions

L929 cells were cultured in the presence or absence of DOPC/DOPE liposomes for 3 days, and the effects of glucose concentrations (i.e., 0, 50, or 1000 μg/ml) in the culture on LD formation was examined. LD formation was determined as fluorescence intensity by flow cytometric analysis after cells were stained using Nile red. As shown in Fig.1, in comparison with the fluorescence intensity of cells before culture (i.e., control defined as 1.0) that of cells cultured in the medium containing 1 mg/ml of glucose was 1.6. After culture in the absence or presence of low-does glucose (50 μg/ml), almost all of the cells died. However, cells cultured in the medium containing both 50 μg/ml of glucose and DOPC/DOPE liposomes (500 µg/ml) were alive and LD induction was detected (i.e., fluorescence intensity of 2.3). Induction of LDs by the liposomes was higher (i.e., fluorescent intensity of 3.7) in culture with high-dose glucose than in that with low-dose glucose. These results suggested that glucose is necessary for liposomes to induce efficiently LDs in cells.

4.4.2. Effect of liposomes on promotion of cell survival

To confirm the effects of the liposomes on cell survival in culture containing low-dose glucose, L929 cells were cultured with or without glucose (50 μg/ml), and various concentrations of liposomes (i.e., 0, 125, 250, and 500 μg/ml) were added to the culture. After culture for 1-3 days, cell viability was determined by a trypan blue dye exclusion test (Fig. 2). In the absence of glucose, cell viability decreased rapidly and almost all of

cells were died after culture for 3 days. Addition of liposomes did not show evident promotion of cell survival in the absence of glucose. In contrast, in the presence of low-dose glucose, cell viability was maintained by the addition of the liposomes in a dose-dependent manner. These results suggest that to exhibit promotion of cell survival, liposomes require a low concentration of glucose in the culture.

To more precisely effects of liposomes on cell survival, L929 cells were cultured in the medium containing a low concentration of glucose for 5 days and cell viability and apoptosis were assessed by the staining of propidium iodide and FAM-FLICA (Fig. 2A) respectively. Propidium iodide does not pass through the cell membrane of living cells while FAM-FLICA is a reagent to detect apoptotic cells. Viable cells were therefore defined as being double negative for propidium iodine and FAM-FLICA staining (i.e., Q4 region of each picture in Fig. 3A). In culture with enough glucose (Fig. 3A(a)), i.e., 1000 µg/ml, cell viability (94.1%) after culture for 5 days was almost equal to that (93.3%) before starting culture (Fig. 3A(e)), whereas in the absence of glucose (Fig. 3A(b)), cell viability was declined to 31.6% (Fig. 6A(b)). Because most dead cells were double positive for propidium iodine and FAM-FLICA, it was suggested that apoptotic cell death was mainly caused by glucose deprivation in these cells. However, addition of DOPC/DOPS or DOPC/DOPE liposomes evidently increased cell viabilities up to 64.5 (Fig. 3A(c)) and 70% (Fig. 3 A(d)), respectively. These results indicate that liposomal treatment suppresses apoptotic cell death and promotes cell survival. Low concentrations of glucose slightly promoted cell survival, up to 40.7% of viability (Fig. 3A(f)). Interestingly, combinatorial treatment with low concentration of glucose and DOPC/DOPS or DOPC/DOPE liposomes synergistically enhanced cell viability up to 90.3% (Fig. 3A(g)) and 91.1% (Fig. 3A(h)) respectively. These results suggest that the liposomal effects on cell survival is closely linked to glucose metabolism.

To demonstrate LD induction in cells by liposomal treatments, cell images after culture for 4 days (i.e., one day before the flow cytometric analyses was done), are shown here because most cells in every culture appeared to still be alive and it was easier to observe LD induction. As shown in Fig. 3B(a), (b) and (c), in the absence of liposomes, evident morphological changes showing LD induction in the cells were not observed. In contrast, as shown in Fig. 3B (c), (d), (f) and (g), those showing LD induction (i.e., ring-shaped distributions of LDs) was evidently observed in the cells treated with

DOPC/DOPS or DOPC/DOPE liposomes. These results suggest that LD induction is closely related to the promotion of cell survival by liposomal treatment under glucose-deficient conditions.

4.5 Discussion

In the study described in Chapter II, I showed that PNPs including liposomes can induce LDs in mammalian cells. Organelles consider LDs as nutrient providers when the environment is nutrient deficient. I therefore examined the effect of liposomes on LD formation and the survival of cells under glucose-deficient conditions. However, under complete glucose deprivation, evident effects of liposomes on LD formation and survival of cells were not observed. In culture containing low-dose glucose, liposomes apparently exhibited LD induction and promotion of survival in cells. In an extreme nutrient deficient culture it is interesting that to promote cell survival, cooperation between carbohydrate and lipid metabolism became clear. I presume that to use lipids efficiently as an energy source, the helper action of carbohydrate metabolism would be indispensable.

In cell survival promotion induced by liposomes under glucose-deficient conditions, DOPC/DOPS liposomes showed a stronger activity than DOPC/DOPE liposomes. As I have demonstrated previously, DOPC/DOPS liposomes induce LDs in cells more efficiently than DOPC/DOPE liposomes [8]. Therefore, LD formation and cell survival induced by liposomes appeared to be closely linked. To confirm this presumption, experiments to test whether the suppression of LD formation influences the promotion of cell survival by liposomes will be necessary. As shown in Chapter II and III, liposomes are incorporated into endosomes/lysosomes and these are not directly delivered to LDs. Liposomes incorporated in the cells are considered to be degraded by various enzymes including lipases in the lysosomes. Fatty acids derived from degraded liposomes would be utilized to form LDs as a component. Therefore, incorporated liposomes may contribute to energy metabolism indirectly via LDs.

In Chapter III, I demonstrated that SR-B1 acts as a receptor for DOPC/DOPE liposomes; however, a main receptor responsible for DOPC/DOPS liposomes differed from SR-B1. Therefore, receptors for phospholipids plays a crucial role in both LD

formation and cell survival promotion induced by liposomes. Anyway, a precise mechanism responsible for the enhancement of cell survival under glucose-deficient conditions remains to be elucidated by future studies.

In cells exposed to nutrient deficiency, LDs initiate interaction with some organelles, including mitochondria, and promote energy metabolism [3-7]. It has been reported that the energy supply by contact between LDs and other organelles is regulated by various genes including PAT family genes [3]. By examining changes in the expression of these genes in response to liposomes, one would be able to obtain a clue to clarify a mechanism responsible for the liposomal effects on cell survival via LD formation.

4.6 References

1. Olzmann, J. A. and P. Carvalho. 2018. Dynamics and functions of lipid droplets. Nature reviews. Mol. cell bio. 20:137-155.

2. Cabodevilla, A.G., L. Sánchez-Caballero, E. Nintou, V.G. Boiadjieva, F. Picatoste, A. Gubern, and E. Claro. 2013. Cell survival during complete nutrient deprivation depends on lipid droplet-fueled β-oxidation of fatty acids. J Biol Chem. 288:27777-88.

3. Kaushik, S. and A. M. Cuervo. 2015. Degradation of lipid droplet-associated proteins by chaperone-mediated autophagy facilitates lipolysis. Nat. Cell Biol. 17:759-770.

4. Valm, A. M., S. Cohen, W. R. Legant, J. Melunis, U. Hershberg, E. Wait, A. R. Cohen, M. W. Davidson, E. Betzig and J. Lippincott-Schwartz. 2017. Applying systems-level spectral imaging and analysis to reveal the organelle interactome. Nature. 546:162-167.

5. Rambold, A. S., S. Cohen and J. Lippincott-Schwartz. 2015. Fatty acid trafficking in starved cells: regulation by lipid droplet lipolysis, autophagy, and mitochondrial fusion dynamics. Dev. Cell. 32:678-692.

6. Nguyen, T. B., S. M. Louie, J. R. Daniele, Q. Tran, A. Dillin, R. Zoncu, D. K. Nomura and J. A. Olzmann. 2017. DGAT1-Dependent Lipid Droplet Biogenesis Protects Mitochondrial Function during Starvation-Induced Autophagy. Dev. Cell.

42:9-21 e25.

7. Herms, A., M. Bosch, B. J. Reddy, N. L. Schieber, A. Fajardo, C. Ruperez, A. Fernandez-Vidal, C. Ferguson, C. Rentero, F. Tebar, C. Enrich, R. G. Parton, S. P. Gross and A. Pol. 2015. AMPK activation promotes lipid droplet dispersion on detyrosinated microtubules to increase mitochondrial fatty acid oxidation. Nat. Commun. 6:7176.

8. Fujita K., M. Somiya, S. Kuroda, and S. Hinuma. 2019. Induction of lipid droplets in non-macrophage cells as well as macrophages by liposomes and exosomes. Biochem. Biophys. Res. Commun. 510:184-190.

9. Amano, C., H. Minematsu, K. Fujita, S. Iwashita, M. Adachi, K. Igarashi, and S. Hinuma. 2015. Nanoparticles Containing Curcumin Useful for Suppressing Macrophages In Vivo in Mice. PLoS One. doi: 10.1371/journal.pone.0137207.

10. Fujita, K., Y. Hiramatsu, H. Minematsu, M. Somiya, S. Kuroda, M. Seno, and S. Hinuma. 2016. Release of siRNA from Liposomes Induced by Curcumin. J. Nanotechnology doi: 10.1155/2016/7051523

11. Somiya M., Q. Liu, N. Yoshimoto, M. Iijima, K. Tatematsu, T. Nakai, T. Okajima, K. Kuroki, K. Ueda, and S. Kuroda. 2016. Cellular uptake of hepatitis B virus envelope L particles is independent of sodium taurocholate cotransporting polypeptide, but dependent on heparan sulfate proteoglycan. Virology. 497:23-32.

12. Lodish H., A. Berk, S.L. Zipursky, P. Matsudaira, D. Baltimore, and J. Darnell. 2000. Oxidation of Glucose and Fatty Acids to CO_2. Molecular Cell Biology. 4th edition. Section 16.1

13. Goetzman E.S. 2011. Modeling disorders of fatty acid metabolism in the mouse. Prog Mol Biol Transl Sci. 100:389-417

14. Vidali S., S. Aminzadeh, B. Lambert, T. Rutherford, W. Sperl, B. Kofler, and R.G. Feichtinger. 2015. Mitochondria: The ketogenic diet--A metabolism-based therapy. Int. J. Biochem. Cell Biol. 63:55-59.
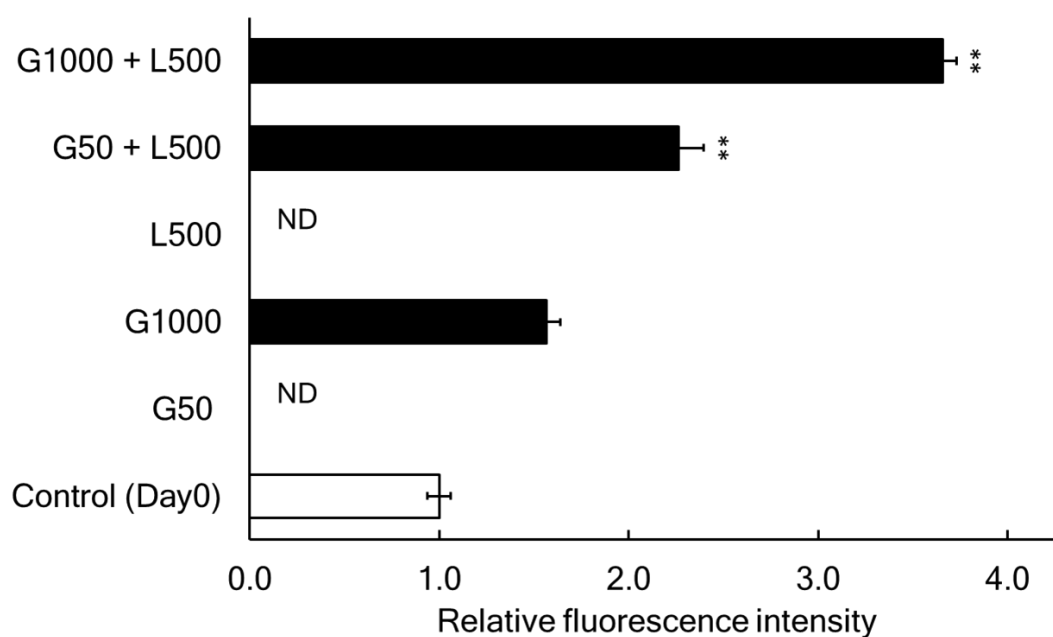
4.7 Figures and legends

Fig.1 Effect of glucose concentrations on LD induction in L929 cells by DOPC/DOPE liposomes. L929 cells were cultured in combination with glucose (50 μg/ml or 1000 μg/ml) and liposomes (500 μg/ml) for 3 days. LDs were stained with Nile Red and detected by a flow cytometer. Data are shown as mean values ± standard errors. Student's t test was performed; ** indicates $p < 0.01$, respectively.
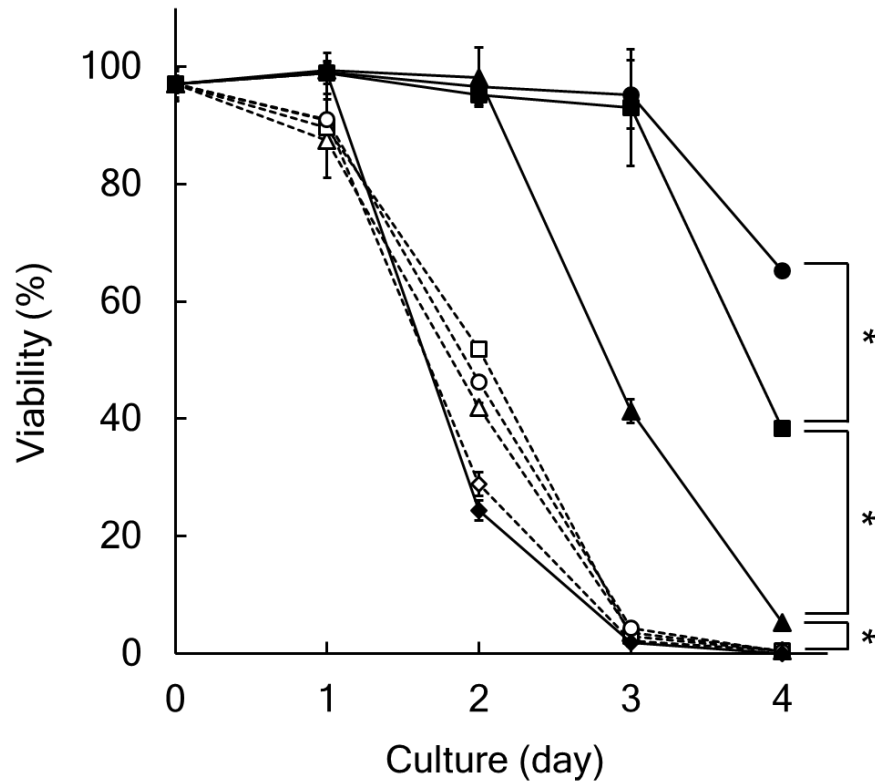
Fig. 2 Enhancement of L929 cell survival by DOPC/DOPE liposomes under low-glucose culture conditions. L929 cells in culture of glucose deprivation were treated with DOPC/DOPE liposomes at the doses of 0 (◇), 125 (△), 250 (□), and 500μg/ml (○). In culture in the presence of 50 μg/ml of glucose, cells were treated with DOPC/DOPE liposomes at the doses of 0 (◆), 125 (▲), 250 (■), and 500μg/ml (●). Cell viability was determined by trypan blue dye exclusion test. Assays were performed in triplicate. Data are shown as mean values ± standard errors. Student's t test was performed; * indicates p < 0.05.
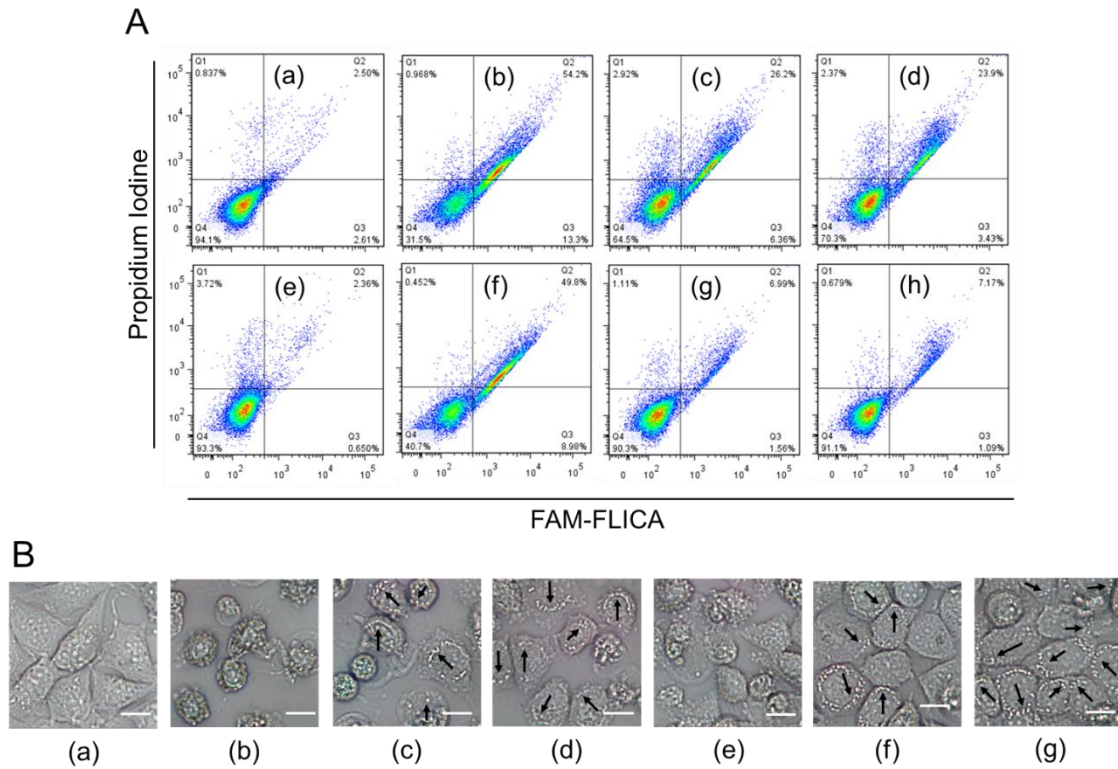
Fig.2 Promotion of L929 cell survival by liposomes under glucose-deficient conditions. A: Cells were cultured for 5 days in the presence or absence of liposomes or glucose. Double staining of propidium iodine and FAM-FLICA was performed, and then the stained cells were analyzed using flow cytometry. Cell culture conditions were as follows; (a): 1000 µg/ml of glucose; (b) none of glucose and liposomes; (c) 25 µg/ml of DOPC/DOPS liposomes; (d) 500 µg/ml of DOPC/DOPE liposomes; (e): before culture of this experiment ; (f): 50 µg/ml of glucose; (g): 50 µg/ml of glucose plus 25 µg/ml of DOPC/DOPS liposomes; (h) 50 µg/ml of glucose plus 500 µg/ml of DOPC/DOPS liposomes. Assays were done in triplicate and a representative result is shown here. B: L929 cells were cultured for 4 days under the same conditions as panel A and their images in culture were captured by inverted microscopy. Cell culture conditions were as follows. (a): 1000 µg/ml of glucose; (b) no glucose or liposomes; (c) 25 µg/ml of DOPC/DOPS liposomes; (d) 500 µg/ml of DOPC/DOPE liposomes; (e): 50 µg/ml of glucose; (f): 50 µg/ml of glucose plus 25 µg/ml of DOPC/DOPS liposomes; (g) 50 µg/ml of glucose plus 500 µg/ml of DOPC/DOPS liposomes. Typical ring-shaped distributions of LDs are indicated by arrow heads. Bars in images indicate 10 µm.

Chapter V

5.1. Concluding remarks

As I referred to the "General introduction" part in this thesis, during the previous studies [1, 2], I noticed that mouse fibroblastic cells (L929) treated with liposomes morphologically changed and granule-like structures appeared in the cytoplasm. This observation led me to initiate the studies in this thesis. Nile red is a lipophilic dye and show fluorescence in a neutral lipid-rich environment. This dye is therefore used to detect lipid droplets (LDs) in cells. Based on Nile red staining, I confirmed firstly that granules induced in cells by liposomes are LDs. BODIPY 493/503 is another fluorescent dye use in the detection of LDs [4]. I could stain granular-like structures induced by liposomes using BODIPY 493/503 too. That is, I could confirm LDs induction by liposomes and exosomes using the two different dyes. LDs were detected by means of flow cytometry and confocal laser microscopy. Later, I confirmed liposome-induced LDs in cells morphologically by transmission electric microscopy [5]. LDs are organelles existing in a wide variety of cells. Adipocytes in animals are specialized cells that store LDs. In adipocytes, LD is formed frequently as a single large LD during maturation. However, in other types of cells, LDs exist as small multiple organelles in the cytoplasm [6, 7, 8, 9].

It has been reported that phospholipid nanoparticles (PNPs), liposomes and exosomes, could efficiently induce LDs in macrophages [10, 11]. LD formation in macrophages have been extensively studied, because abnormal accumulation of LDs in macrophages is closely related to the formation of foam cells in arteriosclerosis. In addition, LDs are related to various diseases [12]. Macrophages are specialized cells that engulf extracellular particles including dead cells and bacteria; they can phagocytose relatively large (i.e., micrometer size) particles [13]. Although phagocytosis of large particles is a characteristic of macrophages, endocytosis of PNPs is recognized ubiquitously in a variety of cells not only macrophages but also non-macrophage cells. However, it has been unknown whether PNPs can induce LDs in non-macrophage cells. Because I have observed that LDs were induced in a non-macrophage cell line by PNPs, I presumed that LD formation would be a common response to PNPs in most mammalian cells. The results of the study on LD induction in various mammalian cells are described in Chapter

II. In this study, I found that all non-macrophage cell lines tested exhibited evident LD induction by PNPs. I confirmed that LDs are induced by PNPs not only in established cell lines but also in primary cultured mouse embryonic fibroblasts (data not shown). Therefore, LD formation in non-macrophage cells induced by PNPs is not a phenomenon restricted to only transformed cells or cancer cells. Through this study, I could prove that LD induction by PNPs is a common response of most mammalian cells. Although its mechanism still remains to be clarified, excessive incorporation of phospholipids into endoplasmic reticulum membranes may stimulate the formation of LDs, because LDs are considered to generate from endoplasmic reticulum membranes [6, 7, 8, 9]. As shown in Chapter II, the triacylgrycelole synthetic pathway appeared to be involved in the induction of LDs by PNPs because triasin C (an acyl-CoA synthetase inhibitor) inhibited the LD induction.

In the study described in Chapter II, the following two results were particularly intriguing. (1) HEK293T cells showed high LD induction comparable to macrophage cell lines in response to PNPs. These results suggest that the ability to endocytose PNPs and some cellular responses to PNPs are not so different between macrophages and non-macrophage cells, although their phagocytic abilities of larger particles are entirely different. (2) Although all liposomes tested with different phospholipid compositions showed LD-inducing activities to HEK293T cells, liposomes containing phosphatidylserine (PS) had greater LD-inducing activity than liposomes containing phosphatidylcholine (PC) and/or phosphatidylethanolamine (PE). I presumed that differential LD-inducing activities of various liposomes reflect different receptors for each phospholipid. That is, PS receptors have a greater ability to induce LDs than PC or PE receptors expressed in HEK293T cells. This presumption comes from the study of phospholipid receptors described in Chapter III. I succeeded in the identification of a receptor for PE, which can induce the efficient endocytosis of PE-containing liposomes. However, in this thesis, eventually, I could not identify PS receptors expressed in HEK293T cells. Transcriptomic data of HEK293T shown in Chapter III suggest that reported PS receptors are unlikely to function in HEK293T cells, because these receptors excluding ANXA5 are weakly expressed [14-16]; I confirmed that ANXA5 does not act as a receptor for the endocytosis of PS-containing liposomes. PS receptors capable of

inducing efficient LD formation in non-macrophage cells therefore remain to be determined by future studies.

In Chapter III, I explained the identification of a receptor for the endocytosis of PE-containing liposomes. After the study in Chapter II was finished, I examined whether LD-induction in HEK293T cells and efficacy of liposomal endocytosis are correlated. However, no correlation was observed between the two events. During these experiments, it was found that PE-containing liposomes are very efficiently incorporated into HEK293T cells. Base on this finding, it was presumed that HEK293T cells would abundantly express receptors for PE, which could induce the efficient endocytosis of PE-containing liposomes. Therefore, HEK293T cells were considered to be an excellent material to search for PE receptors. To find PE receptors expressed in HEK293T cells, I employed a novel approach as follows. I made two simple presumptions: (1) Candidate gene(s) encoding PE receptors would be highly expressed in HEK293T cells and (2) PE receptors would be involved in four receptor families (i.e., reported PE receptors, scavenger receptors, low density lipoprotein receptor family and reported PS receptors) because at least some members of these receptor families have been reported to interact with phospholipids [17]. Based on these two presumptions, I analyzed 52 gene expression levels in transcriptome data of HEK293T cells and narrowed it down to four candidate genes, i.e., ANXA5, SR-B1, LRP3 and SR-B2, in order of high expression levels. CD300A and CD300C were excluded because these genes were weakly expressed in HEK293T cells. To confirm whether these candidate genes encoded PE receptors, I examined the effects of siRNAs against transcripts of these genes. As a result, I found that siRNA against SR-B1, which is known as the primary receptor for high density lipoprotein (HDL), could evidently suppressed DOPC/DOPE liposomal uptake [18-20]. The expression of SR-B1 in HEK293T cells by transfection of a plasmid enhanced DOPC/DOPE liposomal uptake. Treatment of HEK293T cells by anti-SR-B1-antibody could specifically block uptake of DOPC/DOPE liposomes. Additionally, SR-B1-Fc chimeric protein directly bounded to phospholipids including PE. In Chapter II, I showed that PE-containing liposomes can induce LDs in HEK293T cells. This LD induction was abrogated by treatment with SR-B1 siRNA. Therefore, SR-B1 plays a crucial role in both endocytosis and LD formation induced by PE-containing liposomes. After the endocytosis of PE-containing liposomes, these were co-localized with

endosomes/lysosomes and SR-B1. The results of this study unequivocally demonstrate that SR-B1 acts as a receptor to induce the endocytosis of PE-containing liposomes. I expect that the strategy employed in this study to investigate a PE receptor will be applicable to search for receptors for other phospholipids.

In Chapter IV, I showed that PNPs can promote cell survival under glucose-deficient conditions. In culture using normal medium containing sufficient glucose, I observed that treatment of cells with PNPs showed suppressive effects on cell growth (data not shown). PNPs induced LDs in cells in glucose-deficient culture medium as well as the normal medium containing sufficient glucose. I suppose that the three events (i.e., LD induction, promotion of cell survival under nutrient-deficient conditions, and inhibitory effects on cell growth) induced by PNPs are linked together. Future studies are necessary to clarify molecular mechanisms of this linkage.

Through the studies of this thesis, I could clarify at least a part of a mechanism responsible for LD formation in HEK293T cells induced by PE-containing liposomes. In Fig. 1, I illustrated a schematic figure of cellular responses in HEK293T cells induced by PE-containing liposomes. PE liposomes added extracellularly to HEK293T cells selectively bind to a PE receptor (i.e., SR-B1) and perhaps the binding of PE causes a conformational change in SR-B1. PE liposomes bound to SR-B1 are then endocytosed into cells. The endocytosed complex of PE liposomes and SR-B1 facilitate LD formation. In this process, activation of acyl-CoA synthetase is involved. Although Fig. 1 shows an outline of cellular events induced by PE liposomes, some crucial points still remain to be elucidated. In signal transduction, HDL activates a signaling pathway including src family kinases, PI3 kinase, Akt kinase, and MAPK [21]. So far, little is known about signal transduction pathways induced by liposomes. Although my preliminary experiments indicated that PE liposomes stimulate EKR1/2 phosphorylation, I consider that a more detailed analysis of intracellular signal transduction is important to understand the physiological functions of PNPs (data not shown). In this thesis, I succeeded in revealing a PE receptor in HEK293T cells. However, I could not clarify major PC and PS receptors functioning in HEK293T cells. Regarding phospholipid receptors, multiple receptor molecules would exist against a single phospholipid and receptor/ligand combinations would vary depending on cell types and physiological conditions. Therefore, to reveal action mechanisms of PNPs on cellular responses, the approach using liposomes in this

thesis should be useful. I believe that to understand the actions of PNPs on cells and to clarify these mechanisms are very important in the both aspects of basic and applied science.
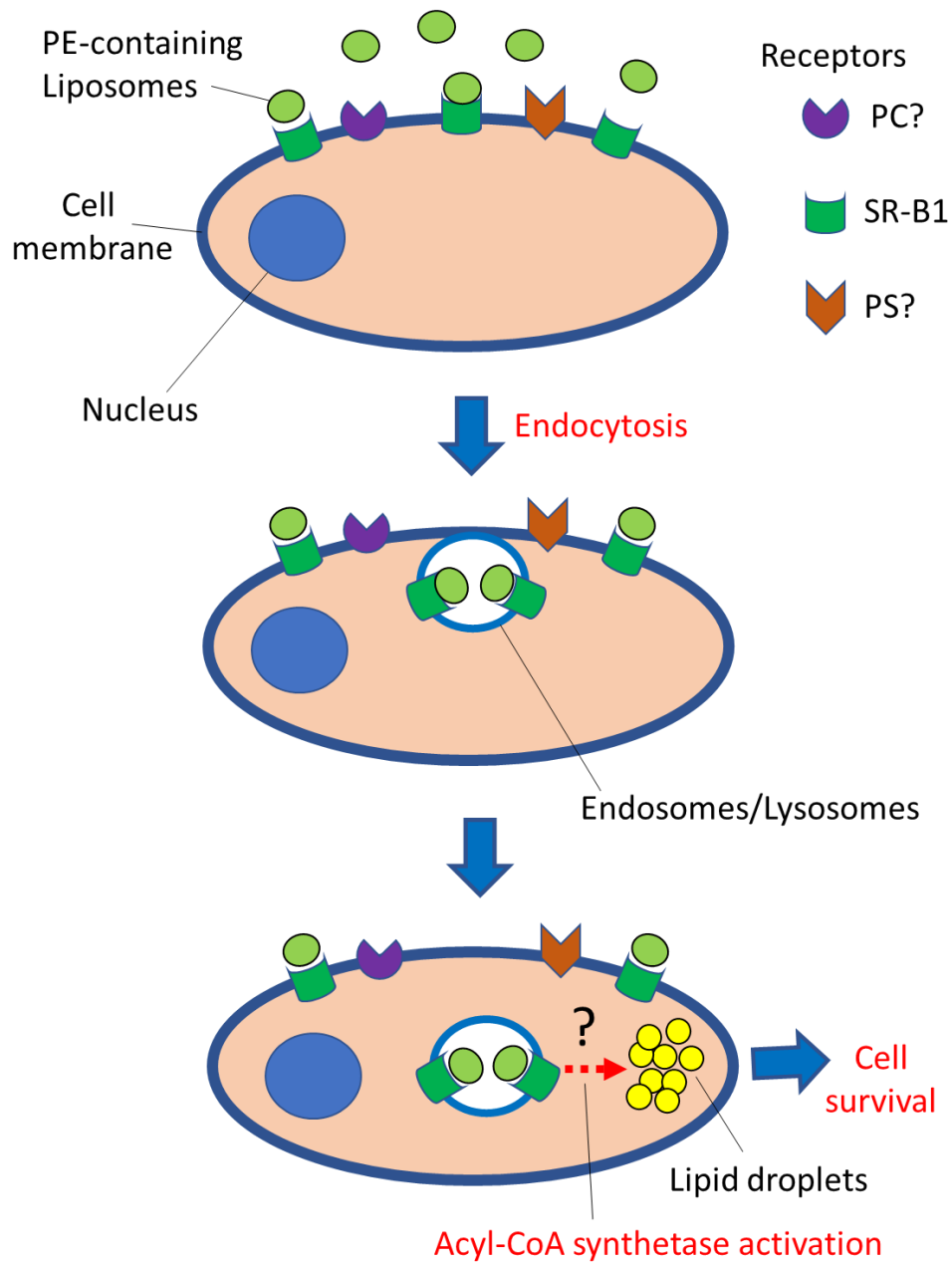

Fig. 1 Cellular responses in HEK293T cells induced by stimulation of PE-containing liposomes.

5.2 References

1. Amano, C., H. Minematsu, K. Fujita, S. Iwashita, M. Adachi, K. Igarashi, and S. Hinuma. 2015. Nanoparticles Containing Curcumin Useful for Suppressing Macrophages In Vivo in Mice. PLoS One. 10:e0137207.

2. Fujita, K., Y. Hiramatsu, H. Minematsu, M. Somiya, S. Kuroda, M. Seno, and S. Hinuma. 2016. Release of siRNA from Liposomes Induced by Curcumin. Journal of Nanotechnology 2016:Article ID 7051523.

3. Greenspan, P., E.P. Mayer, and S.D. Fowler. 1985. Nile red: a selective fluorescent stain for intracellular lipid droplets. J Cell Biol. 100:965-973.

4. Qiu, B., and M.C. Simon. 2016. BODIPY 493/503 Staining of Neutral Lipid Droplets for Microscopy and Quantification by Flow Cytometry. Bio Protoc. 6:e1912.

5. Fujita K., M. Somiya, S. Kuroda, and S. Hinuma. 2019. Induction of lipid droplets in non-macrophage cells as well as macrophages by liposomes and exosomes. Biochem. Biophys. Res. Commun. 10:184-190.

6. Thiam, A.R., R.V.Jr. Farese, and T.C. Walther. 2013. The biophysics and cell biology of lipid droplets. Nat. Rev. Mol. Cell. Biol. 14:775-786.

7. Welte, M.A. and A.P. Gould. 2017. Lipid droplet functions beyond energy storage. Biochim. Biophys. Acta. 1862:1260-1272.

8. Sztalryda, C. and D.L. Brasaemleb. 2017. The perilipin family of lipid droplet proteins: Gatekeepers of intracellular lipolysis. Biochim. Biophys. Acta. 1862:1221-1232.

9. Olzmann, J.A. and P. Carvalho. 2019. Dynamics and functions of lipid droplets. Nature Reviews Mol. Cell Biol. 20:138-155.

10. Nishikawa, K., H. Arai, and K. Inoue. 1990. Scavenger receptor-mediated uptake and metabolism of lipid vesicles containing acidic phospholipids by mouse peritoneal macrophages. J. Biol. Chem. 265:5226-5231.

11. Namatame, I., H. Tomoda, H. Arai, K. Inoue, and S. Omura. 1999. Complete inhibition of mouse macrophage-derived foam cell formation by triacsin C. J. Biochem. 125:319-327.

12. Xu, S., X. Zhang, and P. Liu. 2018. Lipid droplet proteins and metabolic diseases. Biochim. Biophys. Acta Mol. Basis Dis. 1864:1968-1983.

13. Rosales, C. and E. Uribe-Querol. 2017. Phagocytosis: A Fundamental Process in Immunity. Biomed. Res. Int. 2017: 9042851

14. Fadok, V.A., D.L. Bratton, D.M. Rose, A. Pearson, R.A. Ezekewitz, and P.M. Henson. 2000. A receptor for phosphatidylserine-specific clearance of apoptotic cells. Nature. 405:85-90.

15. Zhou, Z. 2007. New phosphatidylserine receptors: clearance of apoptotic cells and more. Dev. Cell. 13:759-760.

16. Armstrong, A.1. and K.S. Ravichandran. 2011. Phosphatidylserine receptors: what is the new RAGE? EMBO Rep. 12:287e288.

17. Penberthy, K.K., and K.S. Ravichandran. 2016. Apoptotic cell recognition receptors and scavenger receptors. Immunol. Rev. 269:44-59.

18. Rigotti, A., S.L. Acton, and M. Krieger. 1995. The class B scavenger receptors SR-BI and CD36 are receptors for anionic phospholipids. J. Biol. Chem. 270:16221-16224.

19. Shen, W.J., S. Asthana, F.B. Kraemer, and S. Azhar. 2018. Scavenger receptor B type 1: expression, molecular regulation, and cholesterol transport function. J. Lipid Res. 59:1114-1131.

20. Gu, X. K. Kozarsky, and M. Krieger. 2000. Scavenger receptor class B, type I-mediated [^{3}H]cholesterol efflux to high and low density lipoproteins is dependent on lipoprotein binding to the receptor. J. Biol. Chem. 275:29993-30001.

21. Seetharam, D., C. Mineo, A.K. Gormley, L.L. Gibson, W. Vongpatanasin, K.L. Chambliss, L.D. Hahner, M.L. Cummings, R.L Kitchens, Y.L. Marcel, D.J. Rader, and P.W. Shaul. 2006. High-density lipoprotein promotes endothelial cell migration and reendothelialization via scavenger receptor-B type I. Circ Res. 98:63-72.

5.3 Acknowledgements

5.4 List of publications

Kazuyo Fujita, Masaharu Somiya, Shun'ichi Kuroda, Shuji Hinuma

Induction of lipid droplets in non-macrophage cells as well as macrophages by liposomes and exosomes.

Biochemical and Biophysical Research Communications (2019) 510(1) p.184-190

5.5 Presentation

藤田和代,曽宮正晴,黒田俊一,日沼州司.

Induction of lipid droplets in non-macrophage cells as well as macrophages by liposomes and exosomes.

第 73 回日本栄養・食糧学会大会、静岡県立大学、2019 年 5 月 18 日(口頭発表)

5.6 Reference related publications

Amano, C., H. Minematsu, K. Fujita, S. Iwashita, M. Adachi, K. Igarashi, and S. Hinuma. 2015. Nanoparticles Containing Curcumin Useful for Suppressing Macrophages In Vivo in Mice. PLoS One. 10:e0137207.

Fujita, K., Y. Hiramatsu, H. Minematsu, M. Somiya, S. Kuroda, M. Seno, and S. Hinuma. 2016. Release of siRNA from Liposomes Induced by Curcumin. Journal of Nanotechnology 2016:Article ID 7051523.